Coupling deformation with fluid flow and mineral reactions based on natural shear zones

–

From field observations to numerical simulations

Dissertation

Submitted in Partial Fulfilment of the Requirements for the Degree

Doktor der Naturwissenschaften (doctor rerum naturalium)

- Lisa Kaatz -

Fachbereich Geowissenschaften

Freie Universität Berlin

Berlin, 2022

Freie Universität Berlin
Department of Earth Sciences

Department of Geological Sciences

Supervisor:

Prof. Dr. Timm John

Prof. Dr. Stefan M. Schmalholz

Submitted by:

Lisa Kaatz

Disputationsdatum: 16.12.2022

Eigenständigkeitserklärung:

Ich erkläre hiermit, dass ich die vorliegende Dissertation selbstständig und ohne unerlaubte Hilfe angefertigt habe. Jegliche verwendeten Hilfsmittel und Quellen sind im Literaturverzeichnis vollständig aufgeführt. Die aus den benutzten Quellen wörtlich oder inhaltlich entnommenen Stellen sind als solche kenntlich gemacht. Des Weiteren erkläre ich, dass die Arbeit bisher weder in gleicher noch in ähnlicher Form einer Prüfungsbehörde vorlag.

Declaration of academic honesty:

I hereby certify that this thesis has been composed by me and is based on my own work, unless stated otherwise. All references have been quoted, and all sources of information have been specifically acknowledged. I further declare that I have not submitted this thesis at any other institution in order to obtain a degree.

_____

Berlin, 31.10.2022

Table of contents

Abstract

At convergent tectonic plate boundaries rocks are brought down into the Earth's mantle. Due to the deep burial, this material is either recycled and contributes to the formation of new and growing orogens or transported further into the mantle. Furthermore, subduction of both oceanic and continental crust assists the Earth's water cycle, which is essential for life on Earth. H_2O bound within the crystal lattice of minerals is brought down into great depth and released by dehydration processes. This released H_2O plays a major role in fluid-rock interaction, since it triggers transformation processes, which subsequently initiate chemical-mechanical changes of the downgoing and surrounding material. Such interdependencies cause metamorphic transition as well as emerging rheological inhomogeneities and deformation of the affected rocks. Especially when dry and rigid rocks of the continental crust are subducted, infiltrating fluids, H_2O in particular, mobilize, promote and increase the efficiency of the chemical-mechanical processes.

How fluid-rock interaction, deformation, rheology, and fluids are coupled and how they affect subducting rocks has long been part of the research. However, investigations of these processes are highly challenging because they occur at great depth where no in-situ analysis is possible. Therefore, studies often use either field-derived data, laboratory data, partially obtained by the analysis of synthetic materials, or complex numerical simulations. This thesis provides a comprehensive dataset arising from detailed field observations and selected samples being analyzed using various methods and equipment. Subsequently, the petrological results were employed for numerical simulations. With this interdisciplinary approach I give new insights into how an infiltrating fluid, mainly H_2O, successively transforms a dry and metastable crustal rock. The fluid infiltration triggers a progressive eclogitization, a transient weakening, and a ductile deformation of the affected host rock. I highlight the role of water, stored in nominally anhydrous minerals (NAMs), which constitute large volumes of the continental crust. Additionally, I present new estimates about the physical-chemical properties, timing, and spatial scales of the addressed metamorphic and dynamic processes.

One of the best natural laboratories to study the transformation and deformation of crustal rocks based on an infiltrating external fluid are the rocks exposed on Holsnøy (western Norway). Various studies have shown that the eclogite-facies shear zone network developed on Holsnøy was formed due to an interplay of brittle and ductile deformation assisted by fluid infiltration. The shear zones widen during strain accumulation, deformation and progressive metamorphism and partially eclogitize the highly reactive granulite. However, it is still a matter of debate how long fluid was available and to what spatial extent. How does it affect the resulting geometries, microstructures and rheology of the system?

To better understand the addressed interconnections, the effect of fluid availability on the evolving shear zone geometry and widening was assed first. The results show that only a substantial amount of fluid enables the geometrical evolution as observed in the field. This fluid was either injected by numerous fluid pulses during individual events or by one large influx. Furthermore, it was possible to decipher that the hydration occurs in two contemporaneous types. By a diffusional hydrogen (H^+/H_2) influx, and simultaneous inflow of an aqueous fluid (H_2O and H^+/H_2). The hydrogen influx caused a hydration of the NAMs, due to an incorporation of OH-groups within the crystal lattice, and progressed further into the wall rock. The supply of H_2O and additional hydrogen through an inflow of aqueous fluid, caused further incorporation of OH-groups during recrystallization into a hydrated eclogite-facies mineral assemblage. Both influxes, where the diffusional hydrogen influx is one order of magnitude faster than the aqueous fluid inflow, initiate a transient weakening of the system. To fit the observed shear zone geometries with numerical simulations, the hydrated granulite must be two orders of magnitude weaker, and the equilibrating eclogite four orders of magnitude weaker compared to the dry and rigid granulite host rock. If inflow of aqueous fluid is modelled only, the eclogite is only three orders of magnitude weaker compared to the granulite. Hence, the hydrogen influx has an appreciable effect on the rheology of the granulite. Furthermore, the conducted numerical simulations provide new time constraints for the granulite hydration and shearing of less than ten years at low shear velocities of $< 10^{-2}$ cm/a. Hence, the results presented here significantly contribute to a better understanding of the fluid-assisted transient weakening and eclogitization of subducted continental crust.

Zusammenfassung

An konvergierenden tektonischen Plattengrenzen wird Gesteinsmaterial subduziert und bis in den Erdmantel gebracht. Jegliches Gesteinsmaterial wird dadurch entweder recycelt und trägt zur Bildung neuer und wachsender Orogene bei oder wird weiter in den Erdmantel transportiert. Darüber hinaus ist die Subduktion der ozeanischen wie auch der kontinentalen Kruste ein signifikanter Bestandteil des Wasserkreislaufs der Erde, welcher für das Leben auf der Erde unerlässlich ist. H_2O, welches gebunden im Kristallgitter von Mineralen vorkommt, wird in große Tiefen befördert und durch Entwässerungsreaktionen freigesetzt. Bei der Wechselwirkung zwischen Fluid und Gestein spielt gelöstes H_2O eine wichtige Rolle, da hierdurch Transformationsprozesse ausgelöst werden, welche anschließend chemisch-mechanische Veränderungen im subduzierten und umgebenden Gesteinsmaterials einleiten. Dazu gehören metamorphe Umwandlungen sowie entstehende rheologische Inhomogenitäten und Verformung der betroffenen Gesteine. Besonders wenn trockene und sogleich rigide Gesteine der kontinentalen Kruste subduziert werden, mobilisieren, fördern und erhöhen infiltrierende Fluide, insbesondere H_2O, die Effizienz der chemisch-mechanischen Prozesse.

Wie Fluid-Gesteins-Wechselwirkungen, Verformung, Rheologie und Fluide miteinander gekoppelt sind und welche Auswirkungen sie auf subduzierende Gesteine haben, ist seit langem Teil der Forschung. Untersuchungen dieser Prozesse sind jedoch sehr anspruchsvoll, da sie in großer Tiefe erfolgen, wo keine In-situ-Analyse möglich ist. Daher beruhen Studien oft entweder auf Felddaten, Labordaten, die teilweise durch die Analyse von synthetischen Materialien gewonnen wurden, oder auf komplexen numerischen Simulationen. Diese Dissertation stellt einen umfassenden Datensatz bereit, der aus detaillierten Feldbeobachtungen und ausgesuchten Proben stammt, welche mit verschiedenen Methoden und Geräten analysiert wurden. Die petrologischen Ergebnissen wurden nachfolgend für numerische Simulationen verwendet. Mit diesem interdisziplinären Ansatz liefere ich neue Einblicke darüber, wie ein Fluid, hauptsächlich H_2O, ein trockenes und metastabiles Krustengestein sukzessive umwandelt. Die Fluidzufuhr löst eine stätig fortschreitende Eklogitisierung, eine vorübergehende Schwächung und duktile Verformung des betroffenen Wirtsgesteins aus. Ich hebe die Rolle von Wasser hervor, welches in nominell wasserfreien Mineralien gespeichert ist, die einen großes Volumen der kontinentalen Kruste ausmachen. Außerdem präsentiere ich neue Abschätzungen über die physikalisch-chemischen Eigenschaften, die Dauer und räumlichen Skalen der angesprochenen Metamorphose- und Verformungsprozesse.

Eines der besten natürlichen Labore, um die Umwandlung und Verformung von Krustengesteinen aufgrund eines externen, infiltrierenden Fluids zu untersuchen, sind die aufgeschlossenen Gesteine auf Holsnøy (West Norwegen). Verschiedene Studien haben gezeigt, dass das auf Holsnøy entwickelte

eklogit-fazielle Scherzonennetzwerk aufgrund des Zusammenspiels zwischen spröder und duktiler Verformung, unterstützt durch eine Fluidzufuhr, gebildet wurde. Die entstandenen Scherzonen verbreitern sich während der Verformung und der fortschreitenden Metamorphose, wodurch eine partielle eklogit-fazielle Rekristallisierung des hochreaktiven Granulits bewirkt wird. Dennoch ist es umstritten, wie lange und in welchem räumlichen Umfang das Fluid zur Verfügung stand. Wie wirkt es sich auf die resultierenden Geometrien, Mikrostrukturen und Rheologie des Systems aus?

Um die angesprochenen Wechselwirkungen besser zu verstehen, wurde zunächst die Auswirkung der Fluidverfügbarkeit auf die entstehende Geometrie und Verbreiterung der Scherzone untersucht. Die Ergebnisse zeigten, dass nur eine beträchtliche Menge an Fluid die im Feld zu beobachtenden Geometrien ermöglichen kann. Entweder wurde das Fluid durch zahlreiche einzelne aufeinanderfolgende Fluideinströmungen injiziert oder durch einen einzelnen erheblichen Zufluss. Weiterhin konnte entschlüsselt werden, dass die Hydratation auf zwei unterschiedlichen Wegen stattfindet. Einmal durch die Zufuhr von Wasserstoff (H^+/H_2), welcher gleichzeitig von einer wässrigen Fluid (H_2O und H^+/H_2) begleitet wird. Der Wasserstoff diffundierte weit in das Nebengestein und bewirkte eine Hydratisierung der nominell wasserfreien Minerale aufgrund des Einbaus von OH-Gruppen in deren Kristallgitter. Die Versorgung mit H_2O und zusätzlichem Wasserstoff durch den Zufluss eines wässrigen Fluids, führte zum weiteren Einbau von OH-Gruppen während der Rekristallisierung in eine folglich wässrige eklogit-fazielle Mineralparagenese. Beide Zuflüsse, bei denen Wasserstoff eine Größenordnung schneller diffundiert als die wässrige Fluide, lösen eine transiente Schwächung des Systems aus. Um die entstandenen Geometrien mit numerischen Simulationen nachbilden zu können, muss der „wässrigere" Granulit um zwei Größenordnungen und der sich equilibrierende Eklogit um vier Größenordnungen schwächer gewesen sein als der trockene und rigide Granulit. Wird nur der Zufluss eines wässrigen Fluids modelliert, so ist der Eklogit nur drei Größenordnungen schwächer als der trockene Granulit. Dies zeigt, dass der Zufluss von Wasserstoff eine deutliche Auswirkung auf die Rheologie des Granulits hat. Die durchgeführten numerischen Simulationen lieferten weiterhin neue Zeitabschätzungen von weniger als zehn Jahren für die Hydratisierung und Scherung des Granulits, mit niedrigen Schergeschwindigkeiten von $< 10^{-2}$ cm/a. Folglich tragen die hier vorgestellten Ergebnisse wesentlich zum besseren Verständnis der fluid-gestützten transienten Schwächung und Eklogitisierung subduzierender kontinentaler Kruste bei.

Chapter 1

Introduction

1.1 Eclogitization of the continental crust

During subduction, the down going plate is exposed to increasing pressure (P) and temperature (T) conditions. Some parts of the slab may be buried into great depth of more than 60 km, where they are expected to transform into eclogite. Discoveries of microdiamonds (e.g., Sobolev and Shatsky 1990; Xu et al. 1992) and coesite (e.g., Smith 1984) in metamorphic rocks even imply burial and eclogitization of continental crust in depths of up to 120 km. However, it is still a matter of debate why or if such deep subductions of continental crust occur, how they influence the movement of tectonic plates, the recycling of elements, exhumation processes, or the formation of orogens.

Usually, eclogites are formed by dehydration of basalt oceanic crust at high (H)P- and low (L)T-conditions (e.g., Eskola 1920; Gao and Klemd 2001; Godard 2001; John et al. 2008; Peacock 1993; Spandler et al. 2003). For these HP-LT-conditions John and Schenk (2003) demonstrated that eclogitization is kinetically delayed (e.g., Rubie 1998; Wayte et al. 1989), if the rocks are dry. Seismic imaging of subducting continental crust reveals a slight bending of the slab accompanied by high seismicity at 80 km depth and below (Figure 1.1, e.g.,Kind et al. 2002; Nábělek et al. 2009; Schneider et al. 2013). It is assumed that this observation is caused by eclogitization (e.g., Andersen et al. 1991b; Marchant and Stampfli 1997). Hence, there is an evidence for kinetically delayed eclogitization of dry and rigid continental crustal rocks, as observed for dry oceanic crust (e.g., John and Schenk 2003).

Due to the buoyancy forces of the continental crust, subduction to eclogite-facies P-T-conditions remains enigmatic. However, various studies demonstrate that subduction of dry crustal rocks is not only possible but influences the deformation, rheology and metamorphic transformation of the down going plate (e.g., Hacker et al. 2010; Raimbourg et al. 2007; Zhang and Green 2007). However, it is unclear if deep subduction of continental crust occurs. Detailed studies on HP and ultra-HP rocks challenge conservative lithostatic pressure calculations and their conclusions about the depth at which these rocks supposedly equilibrated. These P-depth-discrepancies are attributed to tectonic overpressure (e.g., Jamtveit et al. 2018a; Mancktelow 1993; 2008; Schenker et al. 2015; Schmalholz and Podladchikov 2014). In this context, inhomogeneities, e.g., pre-existing microstructures, may lead to variations in P above the lithostatic P (e.g., Mancktelow 1993; Moulas et al. 2019; 2022; Pleuger and Podladchikov 2014; Schmalholz et al. 2014b). Consequently, the formation of an eclogite-facies mineral assemblage may not be caused by deep burial but as a consequence of locally increased P (e.g., Schmalholz et al. 2014a). In either case, dry conditions often force crustal rocks to exist in a metastable state until an externally derived fluid triggers metamorphic reactions (e.g., Beinlich et al. 2020; Jackson et al. 2004).
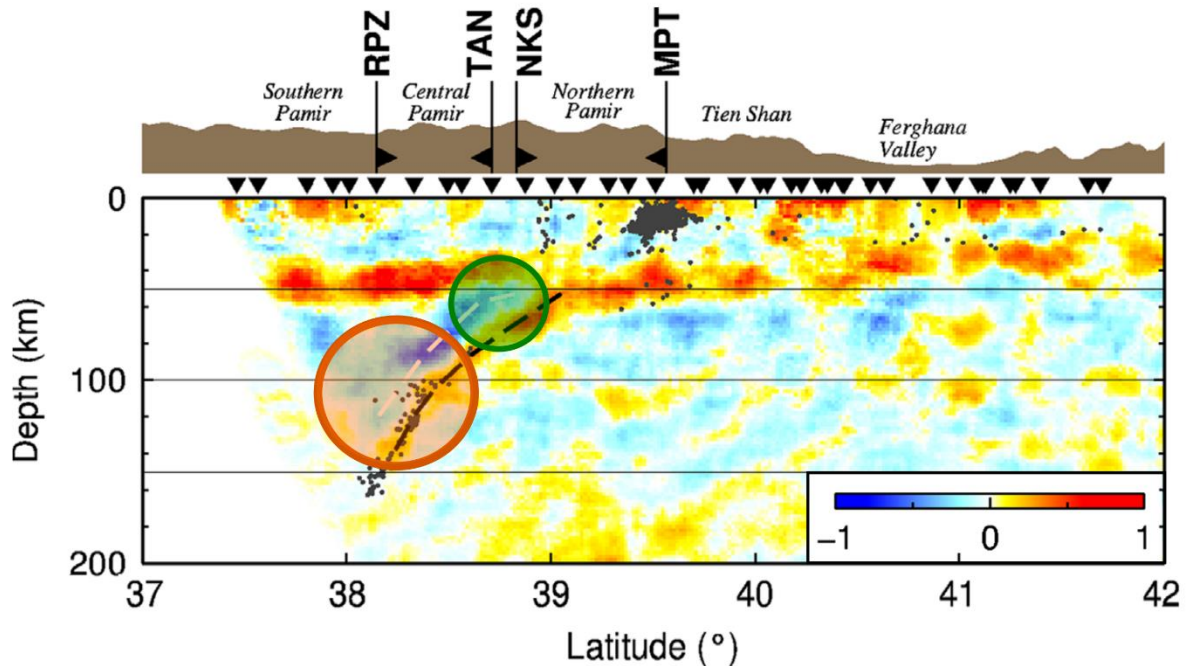
Figure 1.1 An example of an interpreted receiver function image showing subduction of continental crust beneath the Pamir (modified from Schneider et al. 2013). The green circle indicates the area of expected eclogitization (60-70 km depth), associated with the eclogite-facies overprint of wet crustal rocks. The orange circle displays the field of observed kinetically delayed eclogitization for dry crustal rocks. Slab bending, and an evolving invisibility of the slab material accompanies the eclogitization.

As long as the rocks of the continental crust stay dry and rigid during subduction, only brittle deformation enables the infiltration of an externally derived fluid through fractures (e.g., Austrheim 2013; Jamtveit et al. 2018a; Mancktelow and Pennacchioni 2005; Putnis et al. 2017). Once the fluid enters the dry and metastable crustal rock, it lowers the activation energy facilitating mineral reactions (e.g., Milke et al. 2013; Rubie 1986; Zertani et al. 2022a).

1.2 Fluid-assisted eclogitization on Holsnøy

The island of Holsnøy is one of the best natural laboratories to study the fluid-induced eclogitization of dry crustal rocks. The exposures on Holsnøy belong to the Lindås Nappe in Western Norway. The Lindås Nappe itself is part of a tectonic nappe pile forming the Bergen Arc System (e.g., Andersen et al. 1991a; Fossen and Dunlap 1998; Jakob et al. 2017; Roberts 2003). The Lindås Nappe is a section of lower continental crust that originates from the Jotun microcontinent. Before the Caledonian collision this microcontinent was located in the distal part of the hyperextended Baltica margin (e.g., Andersen et al. 2012; Gee and Sturt 1985; Jakob et al. 2019; 2022; Roberts 2003). In addition, this hyperextended domain comprises a basin, which was overthrusted by the Lindås-Jotun nappe complex during the early stage of the Scandian collision (e.g., Andersen et al. 2022; Jakob et al. 2022). Mattey et al. (1994) concluded that the sediments of this basin could be the source of the escaping fluid. Furthermore, partial

melting of schists at the base of the Lindås Nappe is also suggested to contribute to the fluid supply (e.g., Austrheim and Boundy 1994; Jamtveit et al. 2021; Putnis et al. 2017). The infiltrating fluid triggers the eclogite-facies metamorphism of the crustal rocks of the Lindås Nappe at conditions of 670 – 750 °C, and 1.7 – 2.2 GPa at about ~ 430 Ma (e.g., Austrheim 1987, 1998; Bhowany et al. 2018; Fossen 1988; Glodny et al. 2008; Jamtveit et al. 1990; 2018b; Kühn et al. 2002).

The eclogitization and deformation history on Holsnøy can be summarized as follows (Figure 1.2, e.g., Austrheim 1987; Boundy et al. 1992; Bras et al. 2021; Jamtveit et al. 2018a; Jolivet et al. 2005; Labrousse et al. 2010; Raimbourg et al. 2005; Zertani et al. 2019): (i) The metastable granulites were deformed by brittle failure. (ii) Fractures promoted the infiltration of an external fluid, which triggered mineral reactions (Figure 1.2b). (iii) Simultaneously, eclogitization and hydration of the still pristine granulite occurs, forming a hydration halo propagating perpendicular to the precursor-fractures. This halo is temporarily weaker compared to the granulite. (iv) Consequently, strain is localized in the weaker material, causing the formation of eclogite-facies shear zones (Figure 1.2c). (v) During progressive eclogitization and shearing the evolved shear zones propagate, interconnect, and widen. (vi) Hence, a shear zone network is developed, consisting of eclogite-facies shear zones varying in width from some cm up to more than 100 m. However, isolated granulite blocks remain unreacted and internally undeformed (Figure 1.2e). Furthermore, large areas on Holsnøy indicate that eclogitization also occurred statically, which is the eclogite-facies overprint without any associated deformation (Figure 1.2e,f, e.g.,Zertani et al. 2019). Dynamic and static eclogitization interact but develop different field-structures depending on, which process was dominant (Figure 1.2).

In addition, the rocks on Holsnøy were retrogressed at amphibolite-facies conditions (e.g., Austrheim et al. 1997; Centrella 2019; Kühn et al. 2002). Glodny et al. (2008) calculated an amphibolitization age of around 414 Ma. The amphibolite-facies metamorphism proceeded like the eclogitization and partially reactivated present dynamic and static structures. However, based on new age data, Jamtveit et al. (2021) suggests that the time span between eclogitization and amphibolitization is much shorter (< 5 Ma), and not resolvable within the uncertainty of the methods.

Based on this well-established evolution history, it is possible to analyze the underlying processes. For instance, why the eclogite-facies shear zones widen over time during progressive shearing, even though it is commonly suggested that weak shear zones localize the strain and thin (e.g., Poirier 1980). Possible reasons for the shear zone widening are various, e.g., viscosity drop within the wall rock, folding or competent features within the shear zone, grain-size coarsening within the shear zone center or drying of the shear zone (e.g., Finch et al. 2016; Fossen and Cavalcante 2017; Rykkelid and Fossen 1992). Another limiting factor influencing the shear zone widening possibility is the fluid availability and

amount, which is delivered during shear zone formation. It is still a matter of debate to what extent fluid was available to generate the shear zone network exposed on Holsnøy. However, only a few studies decipher and discuss the thickness-displacement-fluid relationship within shear zones (e.g., Menegon et al. 2017; Pennacchioni and Mancktelow 2018).
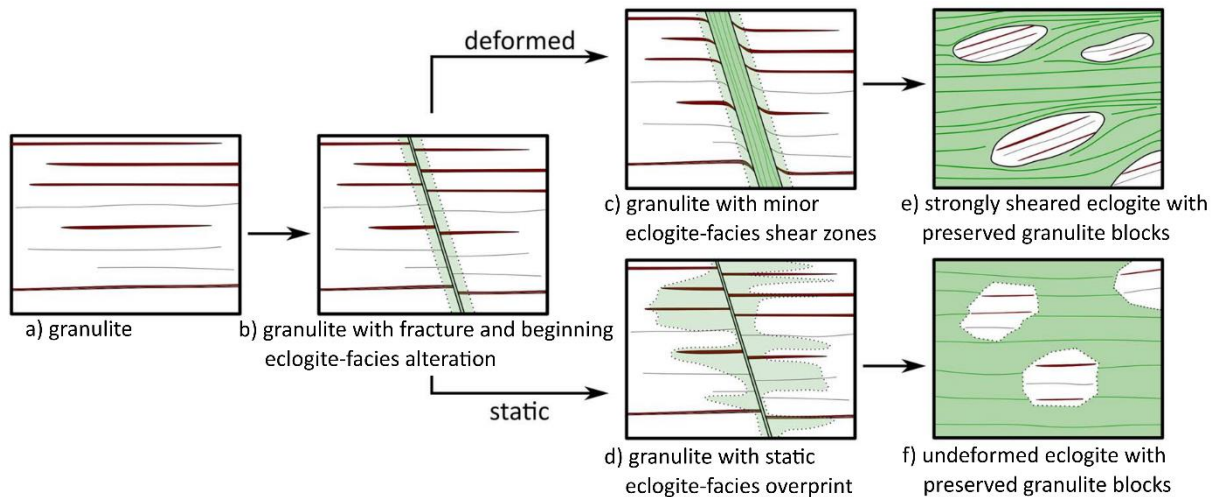
Figure 1.2 Schematic sketches of the dynamic (a,b,c,e) and static (a,b,d,f) eclogitization on Holsnøy (from Zertani et al. 2019). The granulite (a) is fractured (b), which enabled fluid infiltration along this fracture. Eclogite-facies shear zones develop (c) up to a strongly sheared eclogite with preserved granulite blocks (e). Simultaneous static overprint perpendicular to the fracture (d) progressively transformed the wall rock (f).

Another observation is the survival of almost pristine and undeformed granulite blocks (Figure 1.2e, f). Assuming static and dynamic eclogitization to interact, it seems unrealistic that such a highly reactive system stops equilibrating. Different approaches have been made to explain the maintained metastability of the granulites including, local P variations influencing the metamorphic mineral reaction (e.g., Jamtveit et al. 2018b; Mancktelow 2008; Putnis et al. 2021; Wintsch 1985), cool-crust models, where temperature variations inhibit equilibration (e.g., Camacho et al. 2005), and diverse distribution of the fluid biased by an inhomogeneous stress evolution (e.g., Mukai et al. 2014; Yonkee et al. 2003). If stresses drop, and shear zones stop evolving, Oliver (1996) suggested that not consumed fluid is expelled from the shear zone, which is a plausible reason why equilibration of the system may stops. But again, the availability of fluid is probably the limiting factor. This highlights the need for a deeper understanding of how hydration and deformation interact, and of how hydration progressed into the wall rock, e.g., with respect to its spatial distribution.

1.3 Rheological effects caused by fluid infiltration

It is widely accepted that fluid infiltration can weaken initially dry crustal rocks and lead to mineral reactions and thus, changes the bulk rock rheology. Field observation show that fluid-induced and deformation-related weakening may either occurred by a viscosity drop of the wall rock (e.g., Ceccato et al. 2020; Etheridge et al. 1983; Oliot et al. 2010) or due to a strain hardening within the developed shear zone (e.g., Steffen et al. 2001). To increase the viscosity within the shear zone, one possibility is a dynamic recrystallization of coarser grain sizes (e.g., Montési and Hirth 2003). Such processes may be promoted by fluids, affecting the rheology, microstructures and physical properties of crustal rocks, inferring geochemical-rheological feedback mechanisms (e.g., Bedford et al. 2020; Huet et al. 2014; Mancktelow 2002; Schrank et al. 2008; Yamato et al. 2022; Zertani et al. 2022b). Especially, if intensive fluid-rock interaction is present, the strength of the subducting lower crust is reduced (e.g., Fusseis and Handy 2008; Fusseis et al. 2006; Pennacchioni and Mancktelow 2007).

On Holsnøy, transient weakening of the granulitic wall rock is associated with fluid-induced re-equilibration to an eclogite-facies mineral assemblage (e.g., Austrheim 1987; De Ronde et al. 2005; Putnis and Austrheim 2010). During reaction this eclogite is assumed to be weaker but denser, as soon as re-equilibration is completed (e.g., Bras et al. 2021; Malvoisin et al. 2020). Fluid, mainly H_2O, has a large effect on creep mechanisms, e.g., dissolution-precipitation creep, diffusion creep, and dislocation creep (e.g., Brodie and Rutter 1987; John and Schenk 2003; Kohlstedt 2006; Putnis and John 2010; Stünitz et al. 2020), mass transfer, and grain-boundary sliding. Hence, fluid affect the kinetics of mineral reactions (e.g., Ceccato et al. 2022; Tursi 2022). Such processes influence the weakening as well as the deformability of the affected rocks. An immense impact on the processes addressed above, is suggested by the breakdown of plagioclase (plg), which is the most abundant phase in crustal rocks (e.g., Altenberger and Wilhelm 2000; Marti et al. 2018; Menegon et al. 2008; Mukai et al. 2014; Stünitz and Tullis 2001; Tullis and Yund 1985). The study of Zertani et al. (2022a) currently demonstrates that the plg equilibrated rapidly, causing a reaction softening (e.g., Oliot et al. 2010; Rubie 1983), and contribute into the recrystallization of fine-grained, partially hydrous phases (e.g., Gerald and Stünitz 1993; Giuntoli et al. 2018). Consequently, over time, the system is hydrated and gets more prone to ductile deformation. Hence, the plg breakdown is suggested to be one of the key processes for transient weakening and ductile deformation of subducting crustal rocks (e.g., Plümper et al. 2017; Putnis et al. 2021; Wain et al. 2001; Wayte et al. 1989). Somehow, it is still a matter of debate to what extent the fluid-induced weakening occurs, if and how plg facilitates to the weakening. It is rarely quantified what rheological changes are initiated through the fluid-assisted plg breakdown, and how large they were to produce the observed field-structures. Furthermore, duration estimates of such fluid-induced weakening, deformation, and metamorphic transformation processes are rarely available (e.g., Beinlich et al. 2020; Malvoisin et al. 2020) because they are rather short-living.

1.3.1 Nominally anhydrous minerals

Lower crustal rocks typically consist of plg, garnet (grt), quartz (qtz), clinopyroxene (cpx), orthopyroxene (opx), olivine (ol), and alumo-silicates. These phases are nominally anhydrous minerals (NAMs) and incorporate trace amounts of H_2O in the form of OH-groups, where H substitutes for cations (e.g., Bell et al. 1995; Johnson 2006; Kekulawala et al. 1981; Koch-Müller et al. 2004; Rossman 1996; Smyth 2006). It is generally accepted that the P- and T-increase during subduction leads to the breakdown of hydrous phases (dehydration), which releases H_2O as aqueous fluids. These fluids either escape or facilitate mineral reactions. But escaping fluids may promote the hydration of overlaying dry crustal rocks, due to an incorporation of OH-groups within their crystal lattice. This hydration potentially contributes to the weakening of the affected rocks (e.g., Kohlstedt 2006; Tullis et al. 1996). It has been shown for several phases like ol, qtz or grt, that the uptake of water changes the phase properties, weakens the material, and hence, enables ductile deformation of the phases (e.g., Chen et al. 2006; Kekulawala et al. 1981; Mackwell et al. 1985; Xu et al. 2013). However, if and how the hydration of NAMs facilitates to the weakening of subducting lower crustal rocks, is still part of ongoing discussion. Especially on Holsnøy the granulite mineral assemblage mainly constitutes NAMs (e.g., Austrheim 1987), which highlights the need of a deeper understanding how these phases contribute to the hydration and weakening of the entire system.

1.4 Funding of the thesis

This thesis was funded by an Elsa-Neumann grant of the DRS-NaFög (Dahlem Research School-Nachwuchsförderungsgesetz) of Berlin. Additional financial and scientific support was provided by the Deutsche Forschungsgemeinschaft (DFG) through grant 235221301 within CRC 1114 "Scaling Cascades in complex Systems". The thesis was embedded in the subproject C09 – "Dynamics of rock dehydration on multiple scales", which is headed by Marita Christiana Solveig Thomas and Timm John. The goal of CRC 1114 is to understand scaling properties in various disciplines from geology, mathematics to biology, while elaborating a *common language* to solve interdisciplinary questions.

1.5 Aims

This thesis is a cumulative study, which provides new insights to the question of how fluids influence the deformation and metamorphic transformation of dry lower crustal rocks through hydrous shear zones. The aim is to expand the understanding of processes, e.g., widening of the shear zones, transient weakening, metamorphic re-equilibration, and hydration of the crustal wall rock. Especially, the role of NAMs during hydration of the initially dry rocks is analyzed to contribute to the question of how they may influence the rock strength at incipient fluid influx. To do so detailed fieldwork is combined with

laboratory measurements, e.g., electron microprobe microanalyzer (EMPA) and Fourier transform infrared spectroscopy (FTIR). The field-derived observations about the eclogite distribution and shear zone geometries are implemented into numerical simulations. The generated model results are subsequently compared to the natural rocks. Using this approach two outcrops on Holsnøy are investigated to decipher the geometric evolution of the eclogite-facies shear zone network with respect to the fluid availability. Additionally, grt, pyx, and plg of one cm-scale shear zone profile were analyzed to monitor if and how the hydration is recorded in the NAMs of the granulite wall rock. Comprehensive water content measurements and petrological data are used to conduct a second set of numerical simulations. The results provide new insights into viscosity contrasts, the progression of hydration, diffusivity of the fluid, and duration of such processes. Therefore, this thesis contributes to a deeper understanding of processes, which decoding has been part of the scientific debate since decades.

1.5 Structure of the thesis

This thesis is structured into five chapters. Three of them were written as scientific articles, two of which are already published (Chapter 2 and 3), and one is in preparation to be submitted (Chapter 4). The first chapter introduces the overarching topic and current state of knowledge. Furthermore, open questions in the field of fluid-assisted weakening during hydrous shear zone formation and eclogitization of dry crustal rocks are addressed. Chapter five gives a summary of the presented results and an outlook for possible further investigation. For each scientific article chapter supplementary material is given in the appendix. Prior to that, Appendix A lists all articles and conference contributions related to this thesis.

Chapter 2 (published in *Tectonics*, 2021)

This chapter focusses on shear zone widening observed in the crustal rocks exposed on Holsnøy. During fluid infiltration and strain accumulation propagating shear zones partially eclogitize lower crustal rocks. This study aims to get an overview about the originated structures and to identify how fluid availability may influence evolved geometries within the analyzed system. This project was designed by me and Timm John. Field mapping was supported by 3D drone images, which where piloted by Hans Jørgen Kjøll. After a first introductory phase with Loïc Labrousse, Torgeir B. Andersen, Timm John and Sascha Zertani the field mapping of outcrop B was done by me. Outcrop A was mapped by me and Sascha Zertani. Afterwards, I digitized the resulting maps and carried out the EMPA measurements. X-ray fluorescence spectroscopy (XRF) for whole rock analysis were measured at the GFZ Potsdam by Andrea Gottsche. The numerical simulations where prepared and performed by me with the help of Evangelos Moulas and Stefan M. Schmalholz. All authors interpreted the data, were part of the discussion, and commented on previous versions of the article of which I wrote the initial version.

Chapter 3 (published in *Contribution to Mineralogy and Petrology*, 2022)

The study presented in this chapter focuses on the detailed analysis of one representative cm-scale shear zone on Holsnøy. The target was to decipher the role of nominally anhydrous minerals (NAMs) constituting the granulitic wall rock, and the spatial distribution of the eclogite-facies phase abundance. The analyzed NAMs are garnet, clinopyroxene, and plagioclase, which can incorporate several µg/g H_2O, and may record the hydration of the initially dry granulite. The aim is to quantify how and if the NAMs contribute to the hydration and hence, weakening of the system. Me, Timm John and Jörg Hermann designed this project. I collected the sample used for this study. Here, I want to thank Marc Grund, Saskia Bläsing, Timm John who assisted during my field work. The FTIR measurements were performed at the University of Bern with the help of Julien Reynes. Postprocessing and interpreting of the FTIR data were made in cooperation with Jörg Hermann and Julien Reynes. Detailed EMPA measurements and scanning electron microscopy were performed by me. Here, I want to acknowledge Moritz Liesegang and Hans Vrijmoed for technical support. Finally, I collected and combined all data and interpreted the findings together with all coauthors. All of them participated in the discussions and commented on previous versions of the manuscript leading to the final version presented here. The initial draft of the manuscript was written by me.

Chapter 4 (in preparation to be submitted to G^3 – *Geochemistry, Geophysics, Geosystems*)

The work shown in this chapter is a continuation of the research presented in chapter 3. The results demonstrate that the granulitic wall rock hydrated due to a successive hydrogen diffusion and inflow of aqueous fluid. The NAMs recorded the hydration and probably play an important role in the transient weakening of the granulite. This study aims to quantify this hypothesis. The target is to reproduce a field-derived dataset using a simple 1D numerical shear zone model. Furthermore, the results should provide new estimates for realistic viscosity differences as well as time scales. This project was designed by me, Timm John, and Stefan M. Schmalholz. I processed the petrological data used for the numerical simulation. The numerical simulation was performed in cooperation with Stefan M. Schmalholz. The viscosity mixing model used for the simulations was provided by the group of Philippe Yamato, Erwan Bras, Marie Baïsset and Loïc Labrousse. The porosity measurements used within this study were conducted by Core Laboratories in Houston, USA. All authors interpreted, discussed and reviewed previous versions of the manuscript and agreed to present this version in chapter 4, of which I wrote the initial draft.

References – Chapter 1

Altenberger U & Wilhelm S (2000) Ductile deformation of K-feldspar in dry eclogite facies shear zones in the Bergen Arcs, Norway. Tectonophysics, 320, 107-121.

Andersen T, Austrheim H & Burke E (1991a) Fluid-induced retrogression of granulites in the Bergen Arcs, Caledonides of W. Norway: Fluid inclusion evidence from amphibolite-facies shear zones. Lithos, 27, 29-42.

Andersen TB, Corfu F, Labrousse L & Osmundsen P-T (2012) Evidence for hyperextension along the pre-Caledonian margin of Baltica. Journal of the Geological Society, 169, 601-612.

Andersen TB, Jakob J, Kjøll HJ & Tegner C (2022) Vestiges of the Pre-Caledonian Passive Margin of Baltica in the Scandinavian Caledonides: Overview, Revisions and Control on the Structure of the Mountain Belt. Geosciences, 12, 57.

Andersen TB, Jamtveit B, Dewey JF & Swensson E (1991b) Subduction and eduction of continental crust: major mechanisms during continent-continent collision and orogenic extensional collapse, a model based on the south Norwegian Caledonides. Terra Nova, 3, 303-310.

Austrheim H (1987) Eclogitization of lower crustal granulites by fluid migration through shear zones. Earth and Planetary Science Letters, 81, 221-232.

---. 1998. Influence of fluid and deformation on metamorphism of the deep crust and consequences for the geodynamics of collision zones. In When continents collide: geodynamics and geochemistry of ultrahigh-pressure rocks, 297-323. Springer, Dordrecht.

--- (2013) Fluid and deformation induced metamorphic processes around Moho beneath continent collision zones: Examples from the exposed root zone of the Caledonian mountain belt, W-Norway. Tectonophysics, 609, 620-635. 10.1016/j.tecto.2013.08.030.

Austrheim H & Boundy TJS (1994) Pseudotachylytes generated during seismic faulting and eclogitization of the deep crust. 265, 82-83.

Austrheim H, Erambert M & Engvik AK (1997) Processing of crust in the root of the Caledonian continental collision zone: the role of eclogitization. Tectonophysics, 273, 129-153.

Bedford JR, Moreno M, Deng Z, Oncken O, Schurr B, John T, Báez JC & Bevis M (2020) Months-long thousand-kilometre-scale wobbling before great subduction earthquakes. Nature, 580, 628-635.

Beinlich A, John T, Vrijmoed JC, Tominaga M, Magna T & Podladchikov YY (2020) Instantaneous rock transformations in the deep crust driven by reactive fluid flow. Nature Geoscience, 13, 307-311.

Bell DR, Ihinger PD & Rossman GR (1995) Quantitative analysis of trace OH in garnet and pyroxenes. American Mineralogist, 80, 465-474.

Bhowany K, Hand M, Clark C, Kelsey D, Reddy S, Pearce M, Tucker N & Morrissey L (2018) Phase equilibria modelling constraints on P–T conditions during fluid catalysed conversion of

granulite to eclogite in the Bergen Arcs, Norway. Journal of Metamorphic Geology, 36, 315-342. https://doi.org/10.1111/jmg.12294.

Boundy T, Fountain D & Austrheim H (1992) Structural development and petrofabrics of eclogite facies shear zones, Bergen Arcs, western Norway: implications for deep crustal deformational processes. Contributions to Mineralogy and Petrology, 10, 127-146.

Bras E, Baïsset M, Yamato P & Labrousse L (2021) Transient weakening during the granulite to eclogite transformation within hydrous shear zones (Holsnøy, Norway). Tectonophysics, 819, 229026.

Brodie K & Rutter E (1987) The role of transiently fine-grained reaction products in syntectonic metamorphism: natural and experimental examples. Canadian Journal of Earth Sciences, 24, 556-564.

Camacho A, Lee JK, Hensen BJ & Braun J (2005) Short-lived orogenic cycles and the eclogitization of cold crust by spasmodic hot fluids. Nature, 435, 1191-1196.

Ceccato A, Goncalves P & Menegon L (2022) On the petrology and microstructures of small-scale ductile shear zones in granitoid rocks: An overview. Journal of Structural Geology, 104667.

Ceccato A, Goncalves P & Pennacchioni G (2020) Temperature, fluid content and rheology of localized ductile shear zones in subsolidus cooling plutons. Journal of Metamorphic Geology, 38, 881-903.

Centrella S (2019) The granulite-to eclogite-and amphibolite-facies transition: a volume and mass transfer study in the Lindås Nappe, Bergen Arcs, west Norway. Geological Society, London, Special Publications, 478, 241-264.

Chen S, Hiraga T & Kohlstedt DL (2006) Water weakening of clinopyroxene in the dislocation creep regime. Journal of Geophysical Research: Solid Earth, 111.

De Ronde A, Stünitz H, Tullis J & Heilbronner R (2005) Reaction-induced weakening of plagioclase–olivine composites. Tectonophysics, 409, 85-106.

Eskola PE (1920) The mineral facies of rocks.

Etheridge M, Wall V & Vernon R (1983) The role of the fluid phase during regional metamorphism and deformation. Journal of metamorphic Geology, 1, 205-226.

Finch MA, Weinberg RF & Hunter NJ (2016) Water loss and the origin of thick ultramylonites. Geology, 44, 599-602.

Fossen H (1988) Metamorphic history in the Bergen Arcs, Norway, as determined from amphibole chemistry. Norsk geologisk tidsskrift, 68, 223-239.

Fossen H & Cavalcante GCG (2017) Shear zones–A review. Earth-Science Reviews, 171, 434-455.

Fossen H & Dunlap WJ (1998) Timing and kinematics of Caledonian thrusting and extensional collapse, southern Norway: evidence from 40Ar/39Ar thermochronology. Journal of structural geology, 20, 765-781. https://doi.org/10.1016/S0191-8141(98)00007-8.

Fusseis F & Handy M (2008) Micromechanisms of shear zone propagation at the brittle–viscous transition. Journal of Structural Geology, 30, 1242-1253.

Fusseis F, Handy MR & Schrank C (2006) Networking of shear zones at the brittle-to-viscous transition (Cap de Creus, NE Spain). Journal of Structural Geology, 28, 1228-1243. 10.1016/j.jsg.2006.03.022.

Gao J & Klemd R (2001) Primary fluids entrapped at blueschist to eclogite transition: evidence from the Tianshan meta-subduction complex in northwestern China. Contributions to Mineralogy and Petrology, 142, 1-14.

Gee DG & Sturt B. 1985. The Caledonide orogen: Scandinavia and related areas. Wiley.

Gerald JF & Stünitz HJT (1993) Deformation of granitoids at low metamorphic grade. I: Reactions and grain size reduction. 221, 269-297.

Giuntoli F, Menegon L & Warren CJ (2018) Replacement reactions and deformation by dissolution and precipitation processes in amphibolites. Journal of Metamorphic Geology, 36, 1263-1286.

Glodny J, Kühn A & Austrheim H (2008) Geochronology of fluid-induced eclogite and amphibolite facies metamorphic reactions in a subduction–collision system, Bergen Arcs, Norway. Contributions to Mineralogy and Petrology, 156, 27-48. http://dx.doi.org/10.1007/s00410-007-0272-y.

Godard G (2001) Eclogites and their geodynamic interpretation: a history. Journal of Geodynamics, 32, 165-203.

Hacker BR, Andersen TB, Johnston S, Kylander-Clark AR, Peterman EM, Walsh EO & Young D (2010) High-temperature deformation during continental-margin subduction & exhumation: The ultrahigh-pressure Western Gneiss Region of Norway. Tectonophysics, 480, 149-171.

Huet B, Yamato P & Grasemann B (2014) The Minimized Power Geometric model: An analytical mixing model for calculating polyphase rock viscosities consistent with experimental data. Journal of Geophysical Research: Solid Earth, 119, 3897-3924.

Jackson JA, Austrheim H, McKenzie D & Priestley K (2004) Metastability, mechanical strength, and the support of mountain belts. Geology, 32. 10.1130/g20397.1.

Jakob J, Alsaif M, Corfu F & Andersen TB (2017) Age and origin of thin discontinuous gneiss sheets in the distal domain of the magma-poor hyperextended pre-Caledonian margin of Baltica, southern Norway. Journal of the Geological Society, 174, 557-571. https://doi.org/10.1144/jgs2016-049.

Jakob J, Andersen TB & Kjøll HJ (2019) A review and reinterpretation of the architecture of the South and South-Central Scandinavian Caledonides—A magma-poor to magma-rich transition and the significance of the reactivation of rift inherited structures. Earth-science reviews, 192. Jakob J, Andersen TB, Mohn G, Kjøll HJ & Beyssac O (2022) A Revised Tectono-Stratigraphic Scheme for the Scandinavian Caledonides and Its Implications for Our Understanding of the Scandian Orogeny. Geol. Soc. Am. Spec. Paper. In New Developments in the Appalachian-Caledonian-Variscan Orogen.

Jamtveit B, Ben-Zion Y, Renard F & Austrheim H (2018a) Earthquake-induced transformation of the lower crust. Nature, 556, 487-491. https://doi.org/10.1029/2018JB016461.

Jamtveit B, Bucher-Nurminen K & Austrheim H (1990) Fluid controlled eclogitization of granulites in deep crustal shear zones, Bergen arcs, Western Norway. Contributions to Mineralogy Petrology, 104, 184-193.

Jamtveit B, Dunkel KG, Petley-Ragan A, Austrheim H, Corfu F & Schmid DW (2021) Rapid fluid-driven transformation of lower continental crust associated with thrust-induced shear heating. Lithos, 396, 106216.

Jamtveit B, Moulas E, Andersen TB, Austrheim H, Corfu F, Petley-Ragan A & Schmalholz SM (2018b) High Pressure Metamorphism Caused by Fluid Induced Weakening of Deep Continental Crust. Scientific reports, 8, 17011. https://doi.org/10.1038/s41598-018-35200-1.

John T, Klemd R, Gao J & Garbe-Schönberg C-D (2008) Trace-element mobilization in slabs due to non steady-state fluid–rock interaction: constraints from an eclogite-facies transport vein in blueschist (Tianshan, China). Lithos, 103, 1-24.

John T & Schenk V (2003) Partial eclogitisation of gabbroic rocks in a late Precambrian subduction zone (Zambia): prograde metamorphism triggered by fluid infiltration. Contributions to Mineralogy and Petrology, 146, 174-191. https://doi.org/10.1007/s00410-003-0492-8.

Johnson EA (2006) Water in nominally anhydrous crustal minerals: speciation, concentration, and geologic significance. Reviews in mineralogy and geochemistry, 62, 117-154. https://doi.org/10.2138/rmg.2006.62.6.

Jolivet L, Raimbourg H, Labrousse L, Avigad D, Leroy Y, Austrheim H & Andersen TB (2005) Softening trigerred by eclogitization, the first step toward exhumation during continental subduction. Earth and Planetary Science Letters, 237, 532-547. https://doi.org/10.1016/j.epsl.2005.06.047.

Kekulawala K, Paterson M & Boland J (1981) An experimental study of the role of water in quartz deformation. Washington DC American Geophysical Union Geophysical Monograph Series, 24, 49-60.

Kind R, Yuan X, Saul J, Nelson D, Sobolev S, Mechie J, Zhao W, Kosarev G, Ni J & Achauer U (2002) Seismic images of crust and upper mantle beneath Tibet: Evidence for Eurasian plate subduction. science, 298, 1219-1221.

Koch-Müller M, Matsyuk SS & Wirth R (2004) Hydroxyl in omphacites and omphacitic clinopyroxenes of upper mantle to lower crustal origin beneath the Siberian platform. American Mineralogist, 89, 921-931. https://doi.org/10.2138/am-2004-0701.

Kohlstedt DL (2006) The role of water in high-temperature rock deformation. Reviews in mineralogy and geochemistry, 62, 377-396. https://doi.org/10.2138/rmg.2006.62.16.

Kühn A, Glodny J, Austrheim H & Råheim A (2002) The Caledonian tectono-metamorphic evolution of the Lindås Nappe: Constraints from U-Pb, Sm-Nd and Rb-Sr ages of granitoid dykes. Norwegian Journal of Geology/Norsk Geologisk Forening, 82, 45-57.

Labrousse L, Hetényi G, Raimbourg H, Jolivet L & Andersen TB (2010) Initiation of crustal-scale thrusts triggered by metamorphic reactions at depth: Insights from a comparison between the Himalayas and Scandinavian Caledonides. Tectonics, 29, n/a-n/a. 10.1029/2009tc002602.

Mackwell S, Kohlstedt D & Paterson M (1985) The role of water in the deformation of olivine single crystals. Journal of Geophysical Research: Solid Earth, 90, 11319-11333.

Malvoisin B, Austrheim H, Hetényi G, Reynes J, Hermann J, Baumgartner LP & Podladchikov YY (2020) Sustainable densification of the deep crust. Geology, 48(7), 673-677.

Mancktelow N (1993) Tectonic overpressure in competent mafic layers and the development of isolated eclogites. Journal of Metamorphic Geology, 11, 801-812.

Mancktelow NS (2002) Finite-element modelling of shear zone development in viscoelastic materials and its implications for localisation of partial melting. Journal of Structural Geology, 24, 1045-1053.

--- (2008) Tectonic pressure: theoretical concepts and modelled examples. Lithos, 103, 149-177.

Mancktelow NS & Pennacchioni G (2005) The control of precursor brittle fracture and fluid–rock interaction on the development of single and paired ductile shear zones. Journal of Structural Geology, 27, 645-661. 10.1016/j.jsg.2004.12.001.

Marchant R & Stampfli G (1997) Subduction of continental crust in the Western Alps. Tectonophysics, 269, 217-235.

Marti S, Stünitz H, Heilbronner R, Plümper O & Kilian R (2018) Syn-kinematic hydration reactions, grain size reduction, and dissolution–precipitation creep in experimentally deformed plagioclase–pyroxene mixtures. Solid Earth, 9, 985-1009.

Mattey D, Jackson D, Harris N & Kelley S (1994) Isotopic constraints on fluid infiltration from an eclogite facies shear zone, Holsenøy, Norway. Journal of Metamorphic Geology, 12, 311-325.

Menegon L, Pennacchioni G, Malaspina N, Harris K & Wood E (2017) Earthquakes as precursors of ductile shear zones in the dry and strong lower crust. Geochemistry, Geophysics, Geosystems, 18, 4356-4374.

Menegon L, Pennacchioni G & Spiess R (2008) Dissolution-precipitation creep of K-feldspar in mid-crustal granite mylonites. Journal of Structural Geology, 30, 565-579.

Milke R, Neusser G, Kolzer K & Wunder B (2013) Very little water is necessary to make a dry solid silicate system wet. Geology, 41, 247-250.

Montési LG & Hirth G (2003) Grain size evolution and the rheology of ductile shear zones: from laboratory experiments to postseismic creep. Earth and Planetary Science Letters, 211, 97-110.

Moulas E, Kaus B & Jamtveit B (2022) Dynamic pressure variations in the lower crust caused by localized fluid-induced weakening. Communications Earth & Environment, 3.

Moulas E, Schmalholz SM, Podladchikov Y, Tajčmanová L, Kostopoulos D & Baumgartner L (2019) Relation between mean stress, thermodynamic, and lithostatic pressure. Journal of Metamorphic Geology, 37, 1-14. 10.1111/jmg.12446.

Mukai H, Austrheim H, Putnis CV & Putnis A (2014) Textural evolution of plagioclase feldspar across a shear zone: implications for deformation mechanism and rock strength. Journal of Petrology, 55, 1457-1477.

Nábělek J, Hetényi G, Vergne J, Sapkota S, Kafle B, Jiang M, Su H, Chen J & Huang B-S (2009) Underplating in the Himalaya-Tibet collision zone revealed by the Hi-CLIMB experiment. Science, 325, 1371-1374.

Oliot E, Goncalves P & Marquer D (2010) Role of plagioclase and reaction softening in a metagranite shear zone at mid-crustal conditions (Gotthard Massif, Swiss Central Alps). Journal of Metamorphic Geology, 28, 849-871.

Oliver N (1996) Review and classification of structural controls on fluid flow during regional metamorphism. Journal of metamorphic Geology, 14, 477-492.

Peacock SM (1993) The importance of blueschist→ eclogite dehydration reactions in subducting oceanic crust. Geological Society of America Bulletin, 105, 684-694.

Pennacchioni G & Mancktelow N (2018) Small-scale ductile shear zones: neither extending, nor thickening, nor narrowing. Earth-Science Reviews, 184, 1-12.

Pennacchioni G & Mancktelow NS (2007) Nucleation and initial growth of a shear zone network within compositionally and structurally heterogeneous granitoids under amphibolite facies conditions. Journal of Structural Geology, 29, 1757-1780.

Pleuger J & Podladchikov Y. 2014. Tectonic overpressure may reconcile the structural and petrological records of the Adula nappe (Central Alps). In EGU General Assembly Conference Abstracts, 15622.

Plümper O, Botan A, Los C, Liu Y, Malthe-Sørenssen A & Jamtveit B (2017) Fluid-driven metamorphism of the continental crust governed by nanoscale fluid flow. Nature geoscience, 10, 685-690.

Poirier J (1980) Shear localization and shear instability in materials in the ductile field. Journal of Structural Geology, 2, 135-142.

Putnis A & Austrheim H (2010) Fluid-induced processes: metasomatism and metamorphism. Geofluids. https://doi.org/10.1111/j.1468-8123.2010.00285.x.

Putnis A, Jamtveit B & Austrheim H (2017) Metamorphic Processes and Seismicity: the Bergen Arcs as a Natural Laboratory. Journal of Petrology, 58, 1871-1898. 10.1093/petrology/egx076.

Putnis A & John T (2010) Replacement processes in the Earth's crust. Elements, 6, 159-164. https://doi.org/10.2113/gselements.6.3.159.

Putnis A, Moore J, Prent AM, Beinlich A & Austrheim H (2021) Preservation of granulite in a partially eclogitized terrane: Metastable phenomena or local pressure variations? Lithos, 106413. https://doi.org/10.1016/j.lithos.2021.106413.

Raimbourg H, Jolivet L, Labrousse L, Leroy Y & Avigad D (2005) Kinematics of syneclogite deformation in the Bergen Arcs, Norway: implications for exhumation mechanisms. Geological Society, London, Special Publications, 243, 175-192. https://doi.org/10.1144/GSL.SP.2005.243.01.13.

Raimbourg H, Jolivet L & Leroy Y (2007) Consequences of progressive eclogitization on crustal exhumation, a mechanical study. Geophysical Journal International, 168, 379-401. 10.1111/j.1365-246X.2006.03130.x.

Roberts D (2003) The Scandinavian Caledonides: event chronology, palaeogeographic settings and likely modern analogues. Tectonophysics, 365, 283-299. https://doi.org/10.1016/S0040-1951(03)00026-X.

Rossman G (1996) Studies of OH in nominally anhydrous minerals. Physics and Chemistry of Minerals, 23, 299-304.

Rubie DC (1983) Reaction-enhanced ductility: The role of solid-solid univariant reactions in deformation of the crust and mantle. Tectonophysics, 96, 331-352.

--- (1986) The catalysis of mineral reactions by water and restrictions on the presence of aqueous fluid during metamorphism. Mineralogical Magazine, 50, 399-415.

--- (1998) Disequilibrium during metamorphism: the role of nucleation kinetics. Geological Society, London, Special Publications, 138, 199-214.

Rykkelid E & Fossen H (1992) Composite fabrics in mid-crustal gneisses: observations from the Øygarden Complex, West Norway Caledonides. Journal of structural geology, 14, 1-9.

Schenker FL, Schmalholz SM, Moulas E, Pleuger J, Baumgartner LP, Podladchikov Y, Vrijmoed J, Buchs N & Müntener O (2015) Current challenges for explaining (ultra) high-pressure tectonism in the Pennine domain of the Central and Western Alps. Journal of metamorphic Geology, 33, 869-886.

Schmalholz SM, Duretz T, Schenker FL & Podladchikov YY (2014a) Kinematics and dynamics of tectonic nappes: 2-D numerical modelling and implications for high and ultra-high pressure tectonism in the Western Alps. Tectonophysics, 631, 160-175.

Schmalholz SM, Medvedev S, Lechmann SM & Podladchikov Y (2014b) Relationship between tectonic overpressure, deviatoric stress, driving force, isostasy and gravitational potential energy. Geophysical Journal International, 197, 680-696. 10.1093/gji/ggu040.

Schmalholz SM & Podladchikov Y (2014) Metamorphism under stress: The problem of relating minerals to depth. Geology, 42**,** 733-734.

Schneider F, Yuan X, Schurr B, Mechie J, Sippl C, Haberland C, Minaev V, Oimahmadov I, Gadoev M & Radjabov N (2013) Seismic imaging of subducting continental lower crust beneath the Pamir. Earth and Planetary Science Letters, 375**,** 101-112.

Schrank CE, Boutelier DA & Cruden AR (2008) The analogue shear zone: From rheology to associated geometry. Journal of Structural Geology, 30**,** 177-193.

Smith DC (1984) Coesite in clinopyroxene in the Caledonides and its implications for geodynamics. Nature, 310**,** 641-644.

Smyth JR (2006) Hydrogen in high pressure silicate and oxide mineral structures. Reviews in Mineralogy and Geochemistry, 62**,** 85-115.

Sobolev N & Shatsky V (1990) Diamond inclusions in garnets from metamorphic rocks: a new environment for diamond formation. Nature, 343**,** 742-746.

Spandler C, Hermann J, Arculus R & Mavrogenes J (2003) Redistribution of trace elements during prograde metamorphism from lawsonite blueschist to eclogite facies; implications for deep subduction-zone processes. Contributions to Mineralogy and Petrology, 146**,** 205-222.

Steffen K, Selverstone J & Brearley A (2001) Episodic weakening and strengthening during synmetamorphic deformation in a deep-crustal shear zone in the Alps. Geological Society, London, Special Publications, 186**,** 141-156.

Stünitz H, Neufeld K, Heilbronner R, Finstad AK, Konopásek J & Mackenzie JR (2020) Transformation weakening: diffusion creep in eclogites as a result of interaction of mineral reactions and deformation. Journal of Structural Geology, 139**,** 104129.

Stünitz H & Tullis J (2001) Weakening and strain localization produced by syn-deformational reaction of plagioclase. International Journal of Earth Sciences, 90**,** 136-148.

Tullis J, Yund R & Farver J (1996) Deformation-enhanced fluid distribution in feldspar aggregates and implications for ductile shear zones. Geology, 24**,** 63-66.

Tullis J & Yund RA (1985) Dynamic recrystallization of feldspar: A mechanism for ductile shear zone formation. Geology, 13**,** 238-241. https://doi.org/10.1130/0091-7613(1985)13%3C238:DROFAM%3E2.0.CO;2.

Tursi F (2022) The key role of µH2O gradients in deciphering microstructures and mineral assemblages of mylonites: Examples from the Calabria polymetamorphic terrane. Mineralogy and Petrology, 116**,** 1-14.

Wain A, Waters D & Austrheim H (2001) Metastability of granulites and processes of eclogitisation in the UHP region of western Norway. Journal of Metamorphic Geology, 19**,** 609-625.

Wayte GJ, Worden RH, Rubie DC & Droop GT (1989) A TEM study of disequilibrium plagioclase breakdown at high pressure: the role of infiltrating fluid. Contributions to Mineralogy and Petrology, 101**,** 426-437.

Wintsch R. 1985. The possible effects of deformation on chemical processes in metamorphic fault zones. In Metamorphic reactions, 251-268. Springer.

Xu L, Mei S, Dixon N, Jin Z, Suzuki AM & Kohlstedt DL (2013) Effect of water on rheological properties of garnet at high temperatures and pressures. Earth and Planetary Science Letters, 379**,** 158-165.

Xu S, Wen S, Yican L, Laili J, Shouyuan J, Okay A & Sengör A (1992) Diamond from the Dabie Shan metamorphic rocks and its implication for tectonic setting. Science, 256**,** 80-82.

Yamato P, Duretz T, Baïsset M & Luisier C (2022) Reaction-induced volume change triggers brittle failure at eclogite facies conditions. Earth and Planetary Science Letters, 584**,** 117520.

Yonkee W, Parry W & Bruhn R (2003) Relations between progressive deformation and fluid-rock interaction during shear-zone growth in a basement-cored thrust sheet, Sevier orogenic belt, Utah. American Journal of Science, 303**,** 1-59.

Zertani S, John T, Brachmann C, Vrijmoed JC & Plümper O (2022a) Reactive fluid flow guided by grain-scale equilibrium reactions during eclogitization of dry crustal rocks. Contributions to Mineralogy and Petrology, 177**,** 1-18.

Zertani S, Labrousse L, John T, Andersen TB & Tilmann F (2019) The interplay of Eclogitization and deformation during deep burial of the lower continental crust—A case study from the Bergen Arcs (Western Norway). Tectonics, 38**,** 898-915.

Zertani S, Pleuger J, Motra HB & John T (2022b) Highly variable petrophysical properties in felsic high-pressure rocks of the continental crust. Lithos, 410**,** 106572.

Zhang J & Green H (2007) Experimental investigation of eclogite rheology and its fabrics at high temperature and pressure. Journal of metamorphic Geology, 25**,** 97-115.

Chapter 2

Widening of hydrous shear zones during incipient eclogitization of metastable dry and rigid lower crust – Holsnøy, Western Norway

Key Points

- Continuous fluid supply causes shear zone widening

- Shear zones widen during strain accumulation

Chapter 3

How fluid infiltrates dry crustal rocks during progressive eclogitization and shear zone formation: insights from H_2O contents in nominally anhydrous minerals

Key Points

- Water in NAMs

- Eclogitization

- Shear zone formation

- Rock weakening

- Fluid-rock interaction

Chapter 4

Transient weakening during shear zone formation by diffusional hydrogen influx and H₂O inflow – from field observation to numerical simulation

Key Points

- Transient weakening of a dry granulite due to simultaneous inflow of H_2O and diffusional influx of hydrogen during shearing.

- Petrological data and water content data are used to reproduce their spatial variation with a 1D shear zone model.

- Hydrogen diffused further into the dry wall rock and positively affects the transient viscosities. It was possible to resemble the shear zone geometries observed in field, if the diffusional influx of hydrogen already weakens the wall rock viscosity around two orders of magnitudes.

Abstract

The rocks exposed on Holsnøy (Bergen Arcs, Norway) indicate progressive fluid infiltration into a dry, metastable granulite and triggered a kinetically delayed eclogitization, a transient weakening during fluid-rock interaction and the formation of shear zones that widen during shearing. However, the relative importance of diffusional hydrogen influx accompanying the grain-boundary-assisted aqueous fluid inflow on the duration of the granulite hydration, the eclogitization, and on the transient weakening during shear zone formation remain unclear. Here, a 1D numerical model of a viscous shear zone validated by petrological and geometrical data is employed to better constrain fluid infiltration efficiencies, the duration of deformation, and the parameters leading to widening and weakening of a natural eclogite-facies shear zone. Measured eclogite-facies mineral phase abundances and measured OH-groups in nominally anhydrous minerals (NAMs) are used to constrain hydration by aqueous fluid inflow and a diffusional hydrogen influx, respectively. Both hydration processes are described with a diffusion equation and affect the effective viscosity. The shear zone kinematics are constrained by the observed shear strain and thickness. The model fits the petrological profiles if the effective hydrogen diffusivity is approximately one order of magnitude higher than the diffusivity for aqueous fluid inflow. Simultaneously, the model fits the observed shear zone geometry if the viscosity ratio between dry granulite and deforming eclogite is ca. 10^4 and between dry granulite and hydrated granulite ca. 10^2. The results suggest shear velocities $< 10^{-2}$ cm/a, hydrogen diffusivities of ca. $10^{-13 \pm 1}$ m^2/s and a shearing duration of < 10 years.

4.1 Introduction

During collision of tectonic plates, descending crustal rocks are metamorphosed accompanying viscous deformation at increasing pressures (P) and temperatures (T) (e.g., Klemd et al. 2011; Schneider et al. 2013; Yuan et al. 2000). However, it is often observed that dry and rigid parts of the crust do neither undergo ductile deformation nor metamorphism during burial as long they are not affected by the influx of an externally derived fluid (e.g., Austrheim 1987; Jackson et al. 2004; Jamtveit et al. 2018b; Jamtveit et al. 2019; John and Schenk 2003; Mancktelow and Pennacchioni 2005; Menegon et al. 2017; Putnis and Austrheim 2010; Putnis and John 2010). Hence, these rocks maintain their metastability during subduction until fluid triggers mineral reactions. The positive effect of fluid on the ability of a rock to equilibrate and deform is well known and documented (e.g., Austrheim 1987; Hobbs et al. 2008; John and Schenk 2003; Katayama and Karato 2008; Pennacchioni and Mancktelow 2007; Putnis 2021; Stünitz et al. 2020).

Findings on Holsnøy (Bergen Arcs, Norway) show that an infiltrating aqueous fluid triggers eclogite-facies equilibration of a metastable dry granulite (e.g., Austrheim 1987; Jolivet et al. 2005; Kaatz et al.

2022; Zertani et al. 2019). Fluid supply through fractures enables effective mineral reactions (e.g., Austrheim 1987; Zertani et al. 2022), which transiently weaken the granulite during re-equilibration, and contributes to its viscous deformability (e.g., Austrheim 1987; Bras et al. 2021; Kaatz et al. 2021; Moulas et al. 2022; Raimbourg et al. 2005). The result is a network of eclogite-facies shear zones of various scales. Recently, Kaatz et al. (2022) demonstrate that the fluid infiltration on Holsnøy occurred via two different types of contemporaneous hydration processes. A fast-pervasive diffusional hydrogen influx, which hydrated the granulite mineral assemblage, is accompanied by a slower inflow of aqueous fluid, which enables mineral reactions and thus, re-equilibration to eclogite-facies conditions. Several authors show that any aqueous fluid and hence, also subduction zone fluids are dissociated, which means they predominantly consist of H_2O and trace amounts of OH^-, H^+, and H_2 (e.g., Manning 2004; Manning and Frezzotti 2020; Piccoli et al. 2019; Zheng and Hermann 2014). Here, the influx of hydrogen is probably much faster and likely more pervasive compared to the H_2O inflow (e.g., Dohmen and Milke 2010; Tollan and Hermann 2019) because the diffusional hydrogen influx is mainly controlled by grain-boundary, but especially volume diffusion through the grain interiors as described in, e.g., Dohmen and Milke (2010). The inflow of H_2O is possibly driven by the high chemical potential of the reactive metastable granulite or by fluid pressure gradients (e.g., Llana-Fúnez et al. 2012; Malvoisin et al. 2015; Plümper et al. 2017).

It has been shown that hydrogen in the crystal lattice indeed reduces the activation energy of creep mechanisms, especially climb, e.g., in olivine (e.g., De Ronde et al. 2005; Mackwell et al. 1990; Mackwell and Kohlstedt 1990). The phases constituting the granulite mineral assemblage are mainly nominally anhydrous minerals (NAMs), where plagioclase (plg) constitutes large volumes. Kaatz et al. (2022) showed that plg breaks down after limited hydrogen incorporation, causing a matrix grain-size reduction along with the formation of hydrated plg. This may contributes to the strain localization and hence, shear zone formation and weakening (e.g., Herwegh et al. 2008). Plg is the most abundant phase in crustal rocks and probably accounts their rheology and hence, deformability (e.g., Behrens 2021; Mosenfelder et al. 2015; Rybacki and Dresen 2000, 2004). It is a feasible assumption that a fast-pervasive hydrogen influx accompanying the inflow of an aqueous fluid might influence the hydration, eclogitization, rheology, and deformation on Holsnøy. But, only few data are available to support or question a positive effect on such processes due to the uptake of hydrogen especially in plg, but as well in other NAMs constituting crustal rocks.

So far, it has been suggested that the fluid infiltration on Holsnøy is mainly a bulk diffusion of aqueous fluid, mainly H_2O, with bulk diffusivities of $D_b = 10^{-16 \pm 1}$ m^2/s (e.g., Bras et al. 2021; Kaatz et al. 2021). Assuming such diffusivities Bras et al. (2021) provides viscosity ratios during progressive shearing, eclogitization, and hydration of $\eta_{transient}/\eta_{granulite} < 1$, and $\eta_{transient}/\eta_{eclogite} < 1$.. However, an additional

hydrogen influx accompanying the H_2O inflow (e.g., Kaatz et al. 2022) might influence how hydration propagates into the wall rock and how it impacts the rheological behavior of the affected rocks. Constrains on how and to what extend the diffusional hydrogen influx changes the petrological rock properties, e.g., effective viscosities of the system, are rare.

Therefore, this study explores the effect of aqueous fluid inflow and additional diffusional hydrogen influx on the weakening and hydration of the granulite. The aim is to quantify how the hydrogen influx affects the effective viscosities during eclogitization and deformation. Furthermore, the target is to decipher how fast both influxes are and to test whether previously published diffusivities might change. Another aim is to quantify the duration of the hydration-deformation process that lead to the formation of a cm-scale shear zone. To do so, a comprehensive dataset of petrological and geometrical data is used as reference to be replicated by a simple 1D numerical shear zone model. Knowledge about a potential hydrogen-induced weakening is crucial to understand the fluid-induced weakening of subducting continental crust.

4.2 Case study: Holsnøy

Holsnøy is located in western Norway and is part of the Bergen Arc System, which was formed during Caledonian orogeny due to the collision of Baltica and Laurentia (e.g., Andersen et al. 1991; Corfu et al. 2014; Fossen and Dunlap 1998; Hacker et al. 2010; Roberts 2003). As a result, a complex structure of subsequently southeastward thrusted tectonic nappes was built mainly composed of middle Proterozoic anorthositic granulite, mangarites, jotunites, and metagabbros (e.g., Austrheim and Griffin 1985; Jakob et al. 2017). These lithologies partially experienced Caledonian eclogite-to-amphibolite-facies metamorphism at ~ 430 ± 3.5 Ma (Glodny et al. 2008) and at conditions of approximately 2 GPa and ~ 700 °C (e.g., Bhowany et al. 2018; Jamtveit et al. 1990).

At the elevated P-T-conditions the dry and granulite-facies host rocks of Holsnøy were fractured, which enabled a very local fluid infiltration (e.g., Austrheim 1987; Jamtveit et al. 2018a; Jamtveit et al. 1990; Petley-Ragan et al. 2018). It has been suggested that the fluid was either derived from sedimentary rocks undergoing devolatilization during the Caledonian orogeny (Andersen et al. 2012; Jakob et al. 2017; Mattey et al. 1994) or by partial melting of schists and anorthositic granulites at the basement of the nappe pile (e.g., Austrheim and Boundy 1994; Jamtveit et al. 2021). Consequently, the fluid infiltration triggered the eclogitization, which mechanically weakened the metastable granulite within discrete zones having the fluid availability as a limiting factor for the eclogite distribution (e.g., Austrheim 1987; Labrousse et al. 2010; Raimbourg et al. 2007b; Zertani et al. 2019).
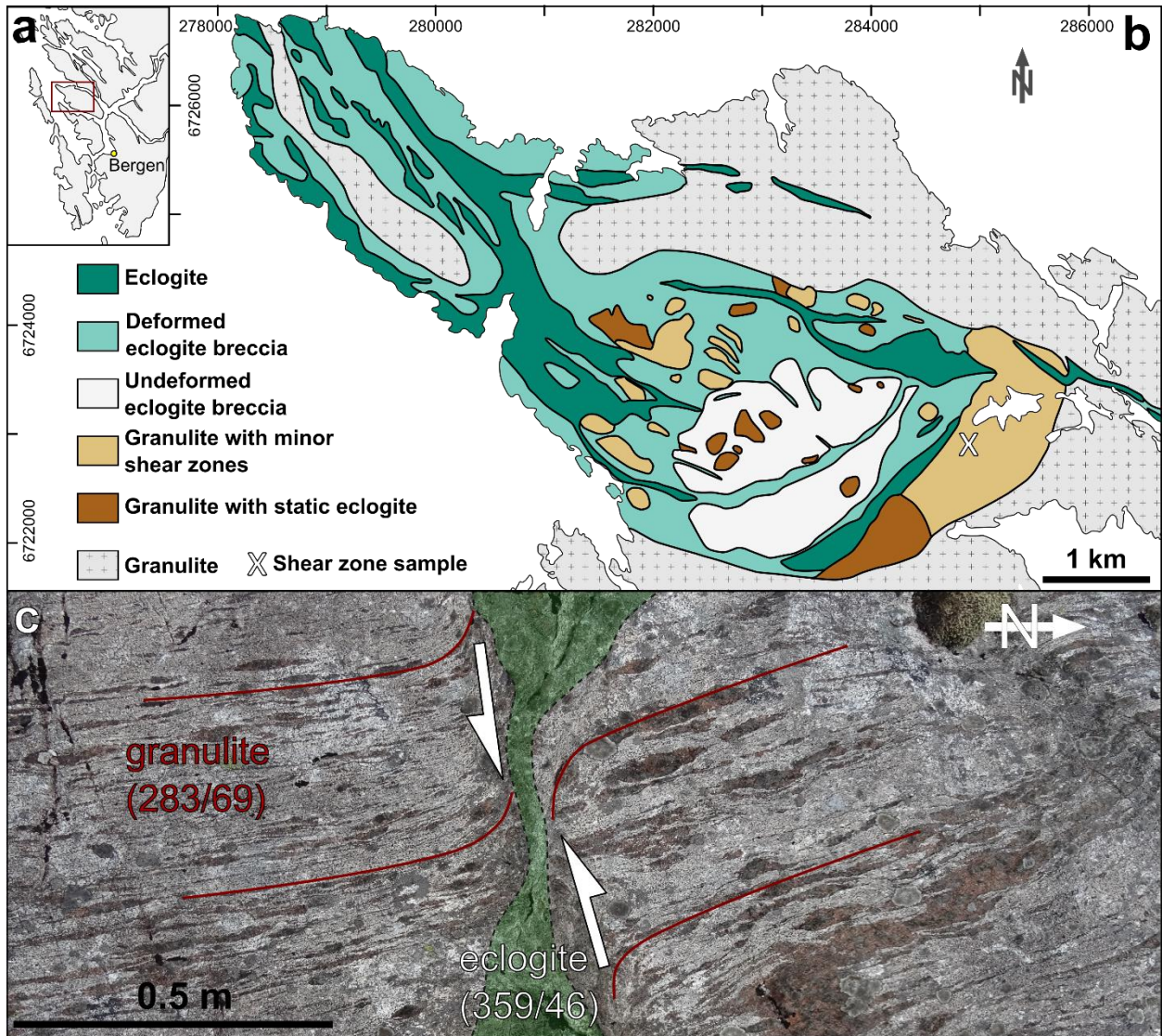
Figure 4.1. (a) Location of northwest Holsnøy northwest of Bergen, Norway (red box). (b) Geological map showing the northwestern part of Holsnøy (modified from Zertani et al. 2022) and its lithological structure with widely distributed eclogitization occurring in various spatial abundances. (c) Photograph of one representative cm-scale eclogite-facies shear zone (highlighted in green, foliation 359/46). Granulite foliation (red lines, foliation 283/69) is dragged into the shear zone indicating dextral sense of shear. Eclogitization is macroscopically limited to the location of the shear zone.

As soon as the granulite was sufficiently weakened the hydrated zones were susceptible to ductile deformation and eclogite-facies shear zones start to form (e.g., Boundy et al. 1992; Kaatz et al. 2021; Putnis and Austrheim 2010; Raimbourg et al. 2005). During progressive deformation the weak shear zones widen due to a sufficient fluid supply and form an interconnected network of small- to large-scale eclogite-facies shear zones (e.g., Austrheim 1987; Fountain et al. 1994; Kaatz et al. 2021). However, large parts were not affected by the pervasive hydration causing an extreme heterogeneous distribution of eclogite abundances (Figure 4.1b, e.g., Austrheim and Griffin 1985; Boundy et al. 1992; Jolivet et al. 2005; Zertani et al. 2019).

4.2.1 Incipient eclogitization of the granulite host rock

The granulite-facies host rock is coarse grained (1 - 5 mm) and mainly composed of pyrope-rich garnet (grt), diopsidic to augitic clinopyroxene (cpx) and labradoritic to andesitic plagioclase (plg) (e.g., Austrheim and Robins 1981; Raimbourg et al. 2007a; Zertani et al. 2019). Grt and cpx are consolidated within elongated coronas, which built a pronounced foliation. The matrix mainly consists of up to 70% plg (e.g., Austrheim and Griffin 1985; Kaatz et al. 2022; Zertani et al. 2019).

The recrystallized eclogite is fine-grained (< 1 mm) and composed of grt, omphacite (omph), clinozoisite (czs), kyanite (ky), and accessory phases, e.g., quartz (qtz), amphibole (amph), phengite (ph, e.g., Austrheim 1987). If a pronounced foliation is present it is produced by aligned omph minerals. The grt has a preserved granulite-facies core and an eclogite-facies almandine-rich rim (e.g., Pollok et al. 2008; Raimbourg et al. 2007a). No plg of granulite-facies composition is left within the eclogite-facies mineral assemblage. The bulk chemistry of granulite and eclogite is similar implying that the fluid composition was quickly rock buffered (e.g., Austrheim 1987).

Using the cross-section sample of Kaatz et al. (2022) with a cm-scale eclogite-facies shear zone and its wall-rock granulite (Figure 4.2a-c) it becomes obvious that the hydration progressively transposes the granulitic host rock by developing different microstructures and grain sizes depending on the distance from the shear zone (Figure 4.3). The following descriptions are mainly based on the analysis of Kaatz et al. (2022) but are very similar to those described by various studies on Holsnøy (e.g., Austrheim 1987; Boundy et al. 1992; Jamtveit et al. 1990; Putnis 2021; Zertani et al. 2019).

The granulite is coarse-grained with grain sizes of approximately 1 mm for grt and plg, and > 2 mm for the cpx (Figure 4.3a,e,i). The grt grains are isometric, have a homogenous composition ($\sim Alm_{29}Pyr_{52}Grs_{19}$), and are often fractured. Cpx (diopsidic to augitic) occurs within coronas and often synergized with grt. Plg ($An_{45}Ab_{54}Or_1$) constitutes ~ 60% of the granulite matrix with distinct phase boundaries (Figure 4.3i).

The transition zone, from eclogite-facies shear zone to dry granulite wall rock, do provide first czs needles, which form along the plg phase boundaries (Figure 4.3j). They are the first result of incipient eclogitization. Correspondingly, hydration cause an immediate reduction of the average matrix grain size of approximately three orders of magnitude (Figures 4.2d). The abundance of the czs needles increase towards the eclogite-facies shear zone, and czs is often intergrown with an albite-rich ($\sim An_{28}Ab_{71}$) plg (e.g., Incel et al. 2019; Petley-Ragan et al. 2018; Zertani et al. 2022). Czs formation is not limited to the former plg phase boundaries but also occurs within the plg grain interior (Figure 4.3k). The grt grains develop an eclogite-facies Fe-rich rim ($\sim Alm_{45}Pyr_{36}Grs_{19}$), and lose their isometric shape

(Figure 4.3b, c), indicating volume loss. Especially within the coronas, when the grt is in contact with plg, a reaction rim is formed mainly composed of omph and czs producing an irregular grt rim with angular grain boundaries of ~120°. This indicates an established equilibrium. The granulite-facies cpx composition is maintained throughout the entire transition zone. With decreasing distance to the shear zone, a reaction rim is formed when the cpx is in contact with plg (Figure 4.3g). This rim comprises amph, czs and omph.

Only a small fraction of relict pristine cpx composition is found at the outer part of the eclogite-facies shear zone. The cpx grain size is reduced to approximately 0.5 mm (Figure 4.3h). The eclogite grt is characterized by irregular rims having a pronounced zonation with a granulite-facies core (~$Alm_{29}Pyr_{52}Grs_{19}$), and an eclogite-facies rim (~$Alm_{45}Pyr_{36}Grs_{19}$). No, plg is left within the eclogite shear zone but the phase is separated into czs, ky, qtz, and amph. These phases have grain sizes of ~10 - 80 µm (Figure 4.3l) in the shear zone, which is an immense contrast to the grain size of the wall rock. The mineral assemblage changed from granulite to eclogite from anhydrous-dominated (< 500 µg/g bulk H_2O) to hydrous (> 2500 µg/g bulk H_2O, Figure 4.2d).
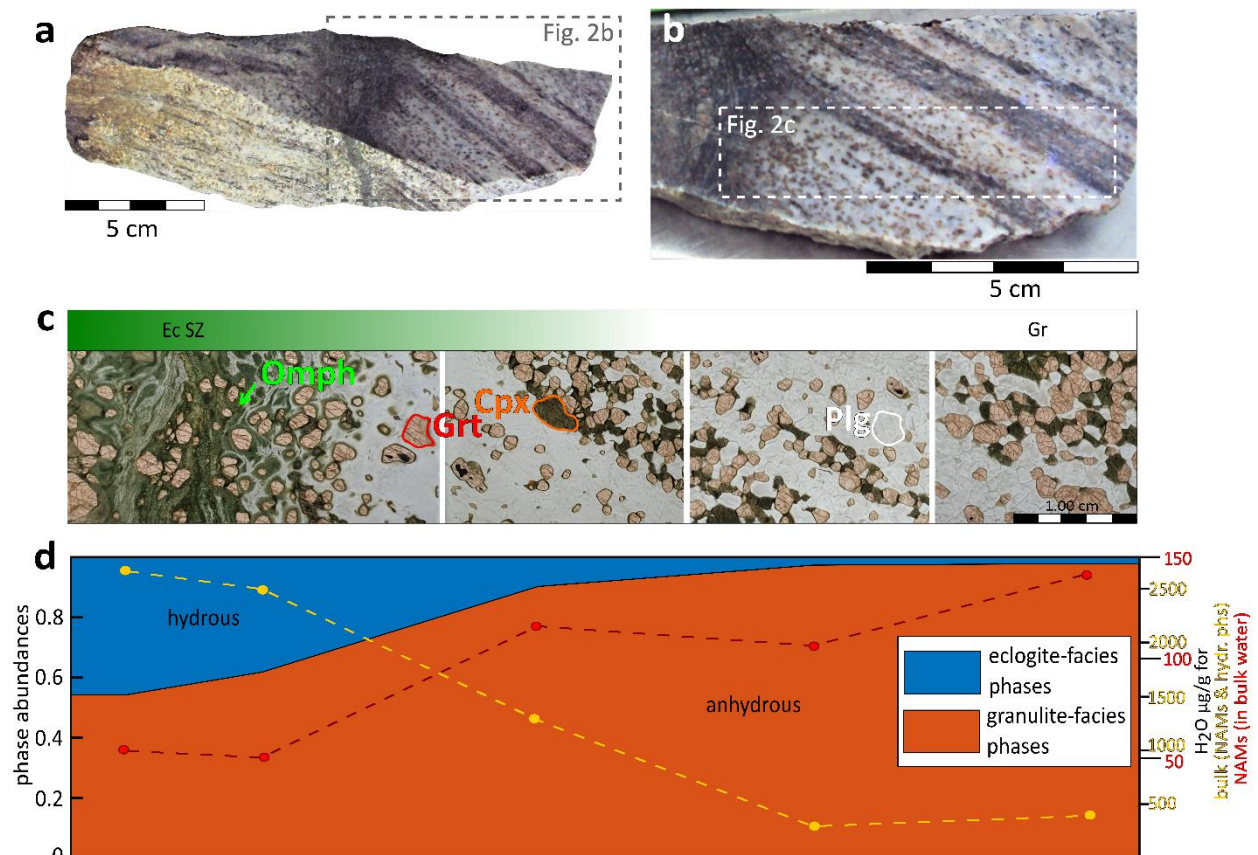
Figure 4.2. (a) Photograph of the sample analyzed in Kaatz et al. (2022) with a cm-scale localized eclogite-facies shear zone in the center surrounded by almost pristine granulite. (b) Rock slice showing the right part of the sample used for detailed measurements. (c) Thick-section profile showing the transition from granulite to eclogite, which is characterized by different microstructures and abundance of eclogite-facies phases. Most abundant phases are

grt, granulitic plg, cpx, and omph. (d) Plot representing the modal abundance of anhydrous, granulite-facies phases (orange), and hydrous phases (blue). The yellow line gives the bulk water content including the NAMs (grt, cpx, plg), czs, and amph based on their modal abundance. Red curve represents the water content of the NAMs as a portion of the bulk water. This simplified profile shows the progressive eclogitization, which accompanied a successive hydration of the granulitic wall rock.

4.2.2 Hydration along the cross-section

The water contents within the constituting minerals increase towards the shear zone within areas of preserved granulite-facies composition from $10 – 50\ \mu g/g$ for grt, $100 – 310\ \mu g/g$ for cpx, and $10 – 144\ \mu gg$ for plg (e.g., Kaatz et al. 2022; Malvoisin et al. 2020). This water increase is primarily characterized by an uptake of hydrogen bonded to the oxygen inside the crystal lattice forming OH-groups by decorating pre-existing defects (e.g., Padrón-Navarta et al. 2014; Stalder et al. 2007; Tollan et al. 2018). The fast transport of hydrogen by grain-boundary and volume diffusion does not necessarily require mineral reactions but probably leads to a pre-weakening of the granulite. Contemporaneously, the slower grain-boundary-assisted inflow of aqueous fluid, enables element transfer and exchange by dissolution-precipitation mechanisms. Hence, the addressed microstructural transformations occur while new eclogite-facies, hydrous minerals form and incorporate OH-groups (e.g., Kaatz et al. 2022; Mukai et al. 2014; Petley-Ragan et al. 2018; Zertani et al. 2019). One aim of this study is to get new insights whether a pre-weakening caused by a hydrogen influx is feasible and how it effects the subsequent inflow of an aqueous fluid.

Hydrous eclogite-facies phases, especially czs, are widely distributed throughout the entire cross-section and not limited to the shear zone (Figure 4.2d and Figure 4.3i-l). Hence, the bulk water content drastically increases towards the shear zone based on the increasing modal abundance of hydrous phases, assuming amph and czs to have 2 wt.% H_2O structurally bonded (e.g., Deer et al. 1997, Figure 4.2d, yellow curve). But in the first place the water uptake of the system is driven by the NAMs, which absorb almost 40% of the bulk water (Figure 4.2d, red curve). However, during eclogitization the OH-incorporation of the system is mainly driven by the hydrous phases.
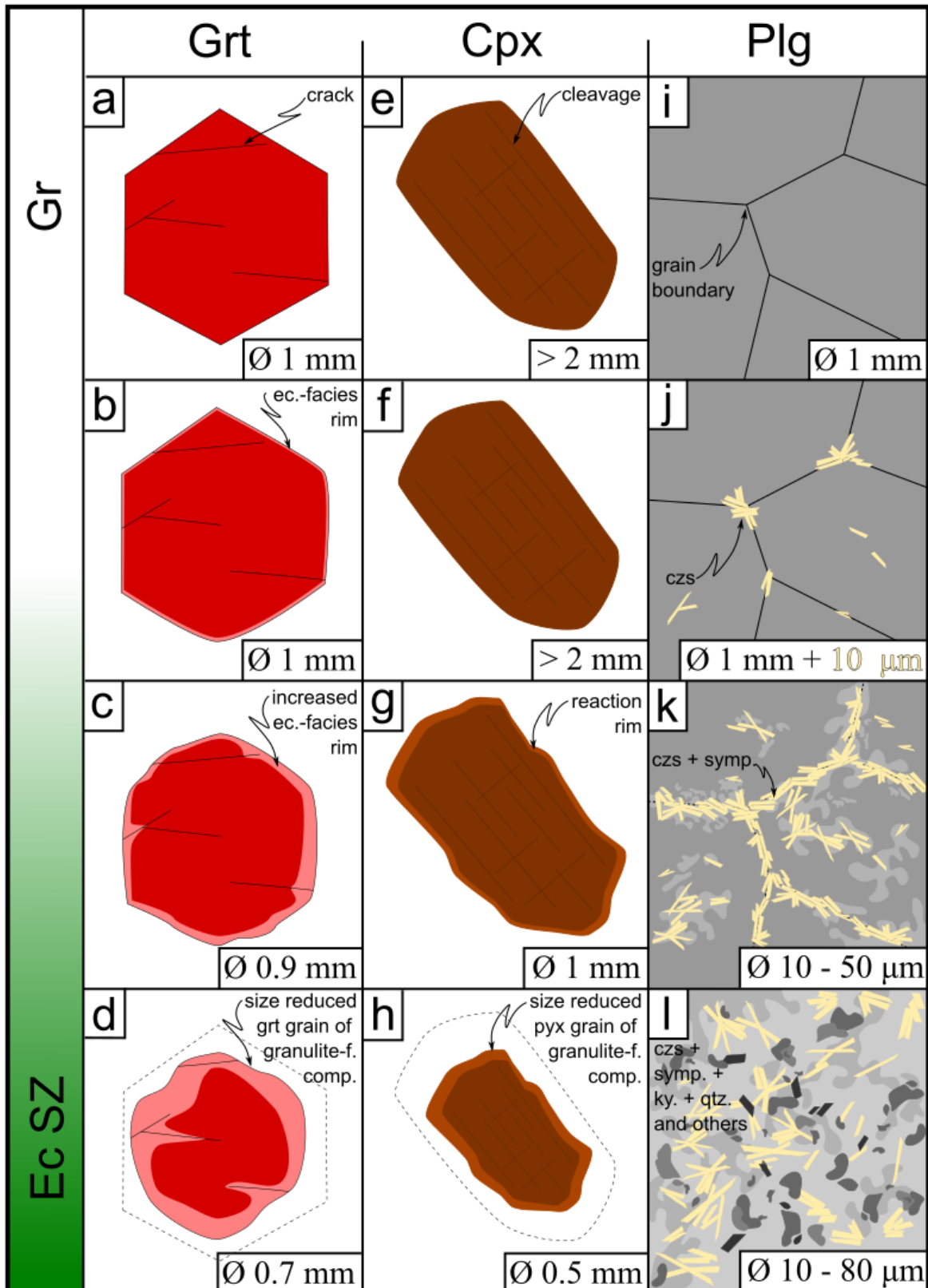
Figure 4.3. Sketch showing the textural and microstructural development for grt (a - d), cpx (e - h), and plg (i - l) from granulite (GrI) to the eclogite-facies shear zone (Ec SZ). During eclogitization grt develops an eclogite-facies Fe-rich rim (light red b - d) while reducing the grain size from approximately 1 mm to 0.7 mm, with a preserved granulite-facies composition within the core (d). Besides the isometric grain shape vanishes and grt develops rims

intergrown with omph in 120° angle at the tens of μm-scale (d). The granulitic cpx has a distinct cleavage (e), and mainly reduce its grain size from > 2 mm to ~ 0.5 mm with decreasing distance to the shear zone by maintained granulite-facies composition (h). The plg underwent the largest changes by complete separation of the phase in close vicinity and within the shear zone. Firstly, czs needles form (j) often building symplectites with an albite-rich plg (k). Secondly, plg of granulite-facies composition is completely replaced by a symplectite consisting of czs, ky, qtz, and amph. This reaction causes a significant grains-size minimization.

4.3 Numerical simulation

A 1D mathematical shear zone model (supplementary material ST4.1) is used to investigate the transient viscosity changes during the fluid-induced shear zone formation. The hydration by aqueous fluid flow and by a diffusional hydrogen influx is described by a diffusion equation. The effective rock viscosity is a function of the hydration. Similar numerical studies have been conducted by Bras et al. (2021) and Kaatz et al. (2021). The model presented here is based on these previous studies, but main elaborations are (1) the consideration of two simultaneous hydration processes by aqueous fluid flow and hydrogen influx and (2) the comparison of both measured petrological and geometrical field data with the results of the numerical simulations. The petrological data consists of two profiles orthogonal to the shear zone indicating the first-order spatial variation of eclogite-facies phase abundance and amount of hydration. The geometrical data consists of the shear zone thickness and the final shear strain.

4.3.1 The mathematical model

To investigate ductile deformation of a rock using numerical models requires a closed system of equations given by the concept of continuums mechanics (e.g., Pollard and Fletcher 2005; Turcotte and Schubert 2014). This set of equations contains (1) conservation equations, including the conservation of mass and of linear momentum (i.e. force balance), (2) constitutive equations, describing the rheological behaviour of a material, e.g., a linear viscous flow, and (3) kinematic equations, e.g., characterizing the relation between velocity and strain rate. A 1D shear zone model (Figure 4.4) is used because it is simple and has a short computation time. The model configuration is dimensionless and scaling of the model results to natural conditions is discussed below.

Viscous simple shear of an incompressible fluid in the absence of gravity is considered (Figure 4.4, e.g., Gerya 2019; Pollard and Fletcher 2005). The conservation of linear momentum for the considered 1D scenario is written as:

$$0 = \frac{\partial \tau}{\partial x} \qquad \qquad (4.\mathbf{I})$$

Here, x is the spatial coordinate and τ is the shear stress. The constitutive equation is (e.g., Gerya 2019):

$$\tau = 2\eta_{eff}\,\dot{\varepsilon} \qquad \qquad (4.\mathbf{II})$$

with η_{eff} being the effective viscosity of the material and $\dot{\varepsilon}$ the shear strain rate. This effective viscosity is a function of the hydration (see below). The shear strain rate is the spatial derivative of the shear velocity (V):

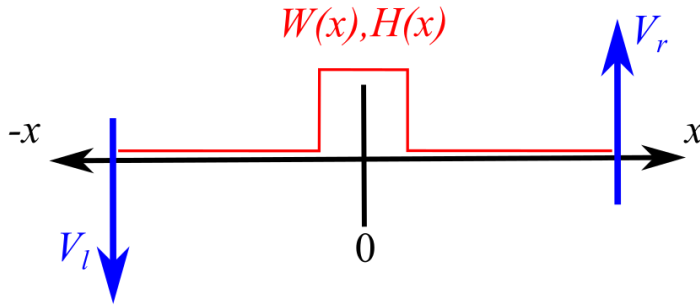$$\dot{\varepsilon} \;=\; \frac{\partial V}{\partial x} \tag{4. III}$$

Figure 4.4. Model configuration for 1D simple dextral shear deformation with a given shear stress τ. Aqueous fluid flow (W) and diffusional hydrogen influx (H) is shown in red. Diffusion perturbates from the center to guarantee symmetry of the process along the x-axis (x, distance).

The hydration is described by a diffusion equation (e.g., Lasaga 1998), which mimics the inflow of H_2O (W) or diffusion of hydrogen (H). For the H_2O inflow, the equation is:

$$\frac{\partial W}{\partial t} \;=\; \frac{\partial}{\partial x}\left(D_w \frac{\partial W}{\partial x}\right) \tag{4. IV}$$

W quantifies the relative progress of eclogitization. $W = 1$ for 100% eclogite-facies mineral phases and $W = 0$ for dry granulite mineral assemblage. D_W represents the effective diffusivity. The same equation is used for the diffusional hydrogen influx, but W is replaced by H and D_W by D_H. H quantifies the relative amount of water in the NAMs representing the uptake of hydrogen. Hence, $H = 0$ for dry granulite, and $H = 1$ for re-equilibrated eclogite, assuming maximum water contents within the shear zone.

The diffusivity of H_2O and hydrogen can be constant or variable. For a variable diffusivity it is assumed that the diffusivity is a non-linear function of W or H. For diffusion of W the following diffusivity is used:

$$D_{W\,non-linear} \;=\; D_W\left[\frac{1 + a}{W + a}\right]^b \tag{4. V}$$

with a and b being fitting parameters, where a defines how much the diffusivity changes between 0 and 1, and b specifies the variation of D_W based on the amount W. The variable diffusivity defined for the hydration of the NAMs, D_H, is based on H, and is described as given in equation (4.IV) but for different values of a and b.

Three end-member viscosities are considered in the model: The dry granulite viscosity $\eta1$, the eclogite

viscosity $\eta 2$ and the viscosity for fully hydrated granulite $\eta 3$ (Table 4.1). Two different hydration scenarios are modelled: single hydration, modelling only the diffusive-type inflow of H_2O, and double hydration, modelling the simultaneous diffusion-type inflow of H_2O and hydrogen influx. For single hydration, the effective viscosity, η_{eff}, is a mixture of $\eta 1$ and $\eta 2$ and the mixing is controlled by the value of W. The so-called Minimized Power Geometric (MPG) mixing model for viscously deforming polyphase rock (Huet et al., 2014) is applied to calculate the value of η_{eff}, as function of $\eta 1$, $\eta 2$ and W. This mixing model has also been applied to eclogite shear zones in granulite by Bras et al. (2021). For double hydration, first an effective viscosity for "hydrated" granulite is calculate from the values of $\eta 1$, $\eta 3$ and H using the MPG mixing model. Then, the value of η_{eff} is calculated from the effective viscosity of "hydrated" granulite, $\eta 2$ and W.

The system of equations described above is solved iteratively using a modified Richardson method, as described by (Halter et al. 2022).

Boundary and initial conditions

The applied dimensionless boundary shear velocities are fixed, being 0.5 on top, and -0.5 at the bottom of the model boundary, and 0 at initial conditions inside the model. Additionally, W and H are fixed to 1 for a restricted area of three grid points in the middle of the shear zone model, representing the eclogite-facies shear zone and fixed to 0 at the model boundaries. The model length was chosen large enough so that the diffusion did not reach the model boundaries at the end of the simulation. The shear strain values derives from displacement calculation for a set of natural shear zones described in Kaatz et al. (2021).

For a first simulation, the following values were used: (1) granulite viscosity $\eta 1 = 1$, (2) viscosity ratios $(\eta 2/\eta 1)$, or $(\eta 3/\eta 2) = 10^1$, (3) $D_W = 10$, and (4) diffusivity ratio $(D_H/D_W) = 2$.

Table 4.1. Abbreviations used in the study.

Explanation	Abbreviation	Units
Effective granulite viscosity	$\eta 1$	Pa.s
Effective eclogite viscosity	$\eta 2$	Pa.s
Effective viscosity of hydrated granulite	$\eta 3$	Pa.s
Aqueous water (H_2O) inflow (eclogite-facies phase abundance)	W	vol.%
Hydrogen influx (OH incorporation in NAMs)	H	µg/g
Diffusivity of H_2O	dW	m^2/s
Diffusivity of hydrogen	dH	m^2/s
Displacement	U	m
Normalized distance (X/shear zone width)	X	m

4.3.2 Natural data for comparison with the model results

To compare changes within the mineral assemblage of the transforming rock and its petrophysical properties, the raw data indicating the fast hydrogen influx (incorporated OH-groups in NAMs, calculated to an H_2O content, supplementary material ST4.2), and the slower inflow of the aqueous fluid (eclogite-facies phases modal abundance, ST4.3) is normalized (Figure 4.5). Normalization means that all values on the y-axis are divided by the maximum value of the specific data set causing a maximum value of 1 for all data sets. The distance orthogonal to the shear zone (x-axis) is normalized by the shear zone thickness to show the onset of the diffusion into the granulitic host rock. This normalization simplifies the comparison between model results and natural data because specific dimensions are absent, and the profiles have the same starting point at both axes. The water contents measured within the NAMs of granulite-facies composition are plotted as normalized data for grt (red), and cpx (blue) in Figure 4.5a, and for the plg (orange) in Figure 4.5b. Grt and cpx together causing a typical smooth profile (dashed line, Figure 4.5a) from the shear zone rim (x-axis 0) to the granulite wall rock (x-axis 5). The plg water contents are plotted separately (Figure 4.5b). Due to phase separation, the granulite-facies plg in close vicinity to the shear zone is either too small to be measured with the FTIR or no reliable signal was detected. Therefore, the data was extrapolated (dotted orange line in Figure 4.5b) from the fitted water content profile (dashed orange line in Figure 4.5b). All water content profiles (grt, cpx, and plg) are finally combined to a single profile (Figure 4.5d blue line). The eclogite-facies phase abundance is illustrated in Figure 4.5c (black dashed line), and characterized by a smooth profile, indicating an increasing abundance of eclogite-facies phases towards the shear zone. The phase abundances are based on several phase maps laterally distributed throughout the sample (Kaatz et al. 2022). Figure 4.5d shows a comparison of both profiles: the bulk water content variation in NAMs (blue line - based on the modal abundance of grt, cpx, and plg), implying a diffusional hydrogen influx, and the variation in eclogite-facies phase abundance (green line), indicating inflow of an aqueous fluid. The two profiles imply that the hydrogen influx progressed further into the wall rock than the H_2O, and hence, was faster, than the aqueous fluid. The profiles shown in Figure 4.5d are used as representative natural profiles for the comparison with results of the numerical simulations.
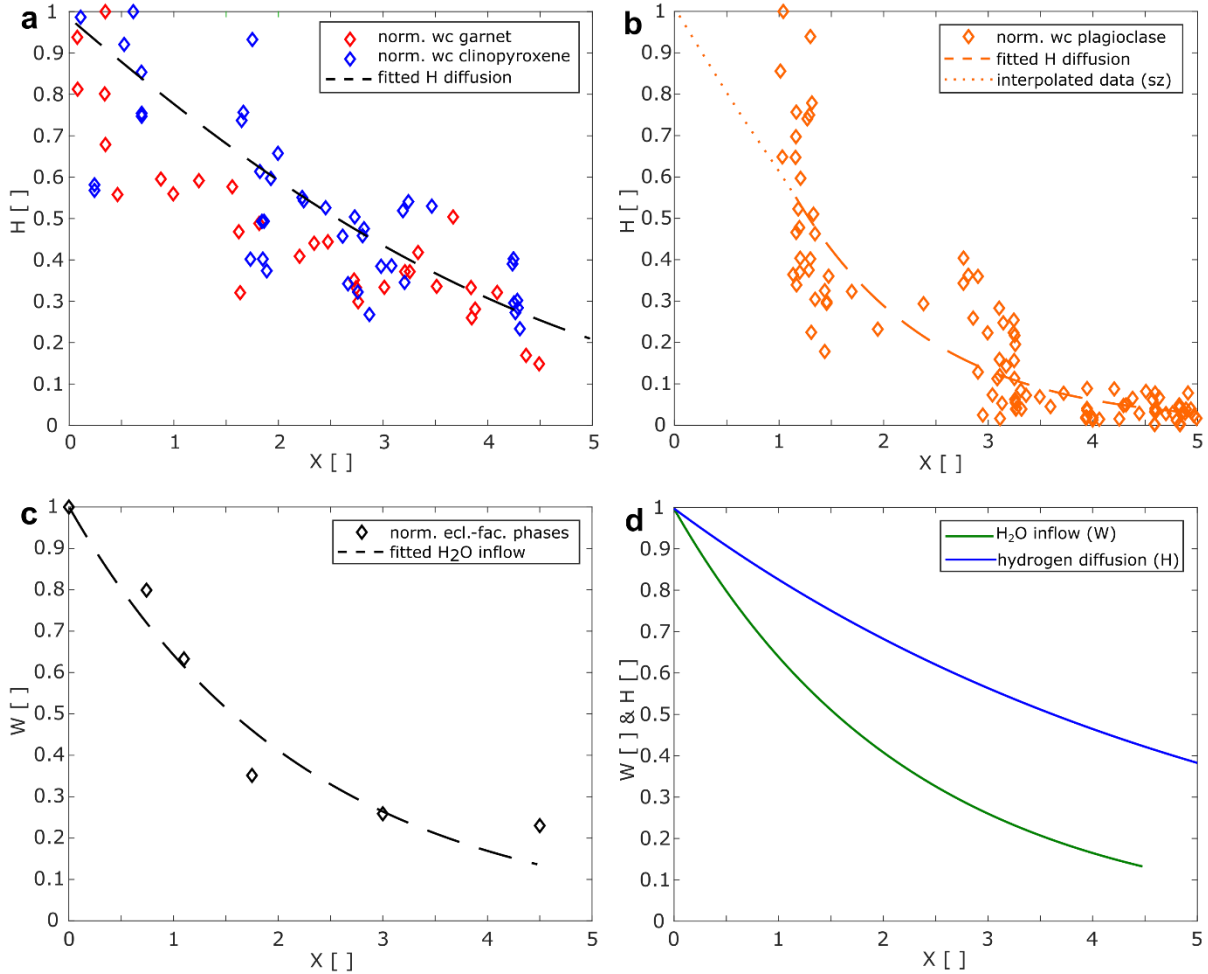
Figure 4.5. (a) Normalized water content data (H []) for garnet (red) and clinopyroxene (blue). One data point represents the average water content measurements of one grain core (granulite-facies composition), which is fitted to a curve (black line), illustrating the hydrogen influx. (b) Normalized water content data (H []) for plagioclase (orange diamonds), representing the average core water content. No plagioclase of pristine granulite composition is left next to the shear zone, causing a data gap between $0 - 1$ (x-axis). The dashed fitted line indicates the hydrogen influx, while the dotted line is an interpolation towards the shear zone. (c) Plotted variation of eclogite-facies phase abundance (black diamonds), where one point represents data of one phase map. The fitted curve illustrates the inflow of an aqueous fluid (W, dashed black line). (d) Comparison of both profiles, fast diffusional hydrogen influx (blue line) and slower inflow of H_2O (green line) along the normalized distance (X []).

4.4 Results

Two types of simulations are performed. At first, single hydration of only H_2O inflow is modelled with a diffusion equation during shear zone formation. For this type of simulation, a first systematic series of simulations with different eclogite viscosity and different, constant diffusivity is performed. The simulation results are compared with the natural data and the best fitting values of eclogite viscosity and diffusivity are determined. For the single hydration simulations, a second systematic series is performed for which the diffusivity is variable and dependent on the amount of H_2O, W (see equation 4.V).

For the second, double hydration type, two diffusion-type hydration processes are considered, which mimic the simultaneous inflow of H_2O and the hydrogen influx.

4.4.1 Single hydration: Fitting the inflow of H_2O – W – Eclogitization

Constant D_W

Figure 4.6 shows representative results for a 1D evolution of the H_2O inflow with constant D_W. After a maximum shear strain of 1 is reached, the simulation stops. For five different shear strains the evolution of the associated normalized displacement (U, Figure 6b), and the effective viscosity ($\eta 2$, Figure 4.6c) is given. Both values depend on the evolution of the strain as well as the shear zone thickness. The shear zone thickness is defined by the shear strain profile across the model. Areas, where the shear strain is higher than the mean shear strain of the system, are defined to belong to the shear zone. The displacement is based on the strain propagation, hence shear zone thickness over time, and cumulatively added after each timestep resulting in the total displacement value. The normalized displacement, U, is the total displacement divided by the final shear zone thickness. Hence, U = γ, for the dimensionless model configuration.

At initial conditions, $\gamma = 0$, η_{eff} is low within the shear zone (Figure 4.6c), because $W = 1$ within the same area. Consequently, both quantities create step-like profiles from shear zone to granulite (Figure 4.6a). As soon as W propagates over time, η_{eff} adjusts as well (cf. 4.6a and 4.6c). U is 0 at $\gamma = 0$ because no shearing occurred so far (Figure 4.6b). If shearing is applied, and the W-profile propagates, U evolves and widen up to a maximum of 1 ($\gamma = 1$), implying shear zone widening based on the distribution of W and shearing.

Variable D_W

A non-linear diffusion, with spatial and temporal variation of D_W according to equation (4.V), enables to adjust the shape of the modelled W-profile. Figure 4.7a displays representative results of the non-linear W-inflow. Initial conditions are the same for constant D_W (cf. Figure 4.6 and Figure 4.7). But, at $\gamma = 0.25$ the gradient of W is higher (blue line Figure 4.7a) compared to a constant D_W (Figure 4.6a), causing a steeper W-profile. However, W and η_{eff} are still interdependent, and if W propagates, η_{eff} changes as well. The normalized displacement U is given in Figure 4.7b, which increased over time with increasing W distribution. Compared to Figure 4.6b, the displacement steps decrease with increasing shear strain but are not constant. The applied values of D_W decreases towards the shear zone (Figure 4.7d).
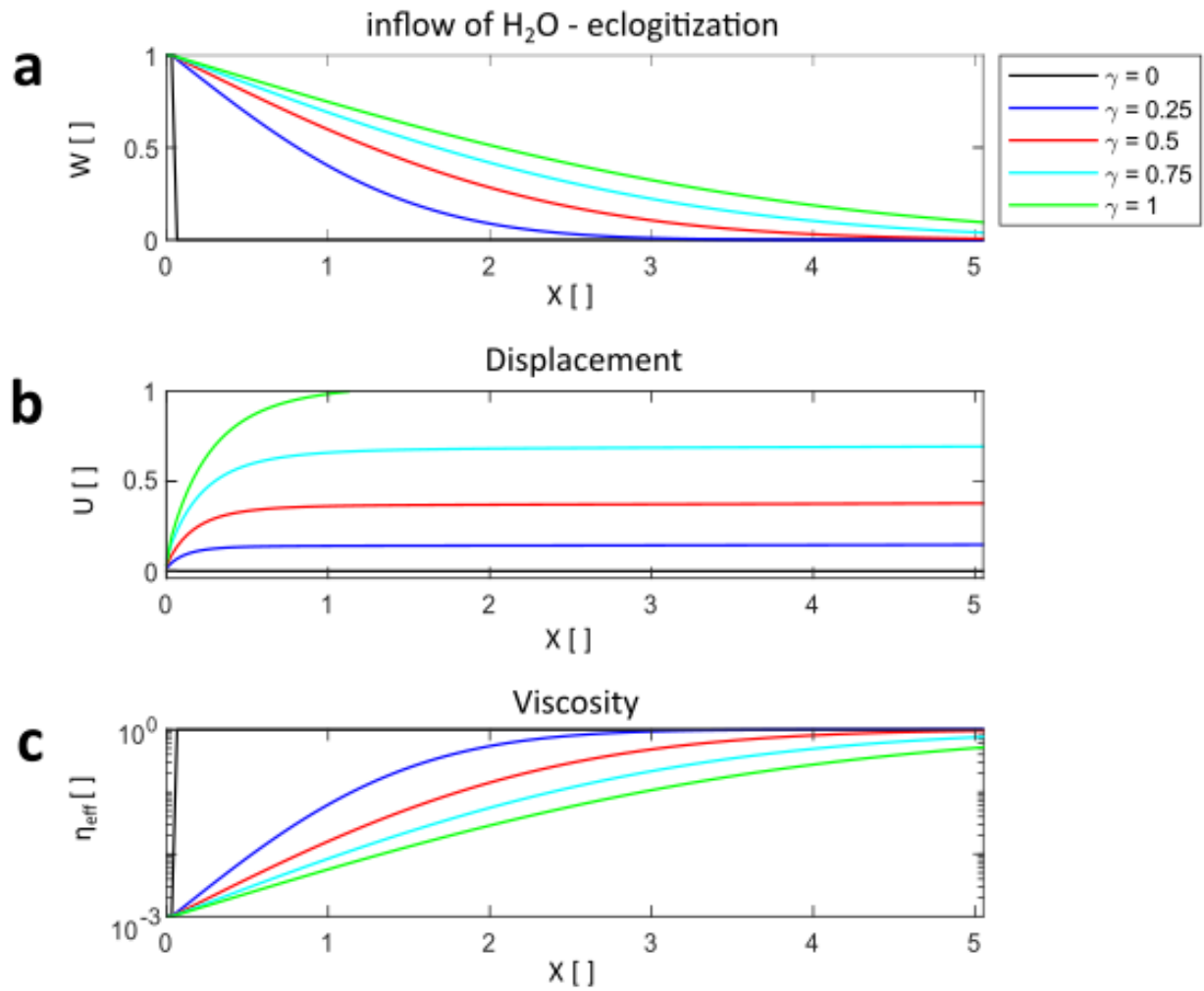
Figure 4.6. Lateral evolution of the H_2O inflow imaging (a) the eclogitization of the system, (b) normalized total displacement, and (c) the effective viscosity for five different shear strains between $\gamma = 0$ and $\gamma = 1$ with a constant D_w. The x-axis is the normalized distance X [ ], which is adjusted by the shear zone width. W [ ] is the amount of eclogitization, U [ ] is the normalized total displacement along the shear zone divided by the shear zone width, and η_{eff} [ ] is the dimensionless effective viscosity.
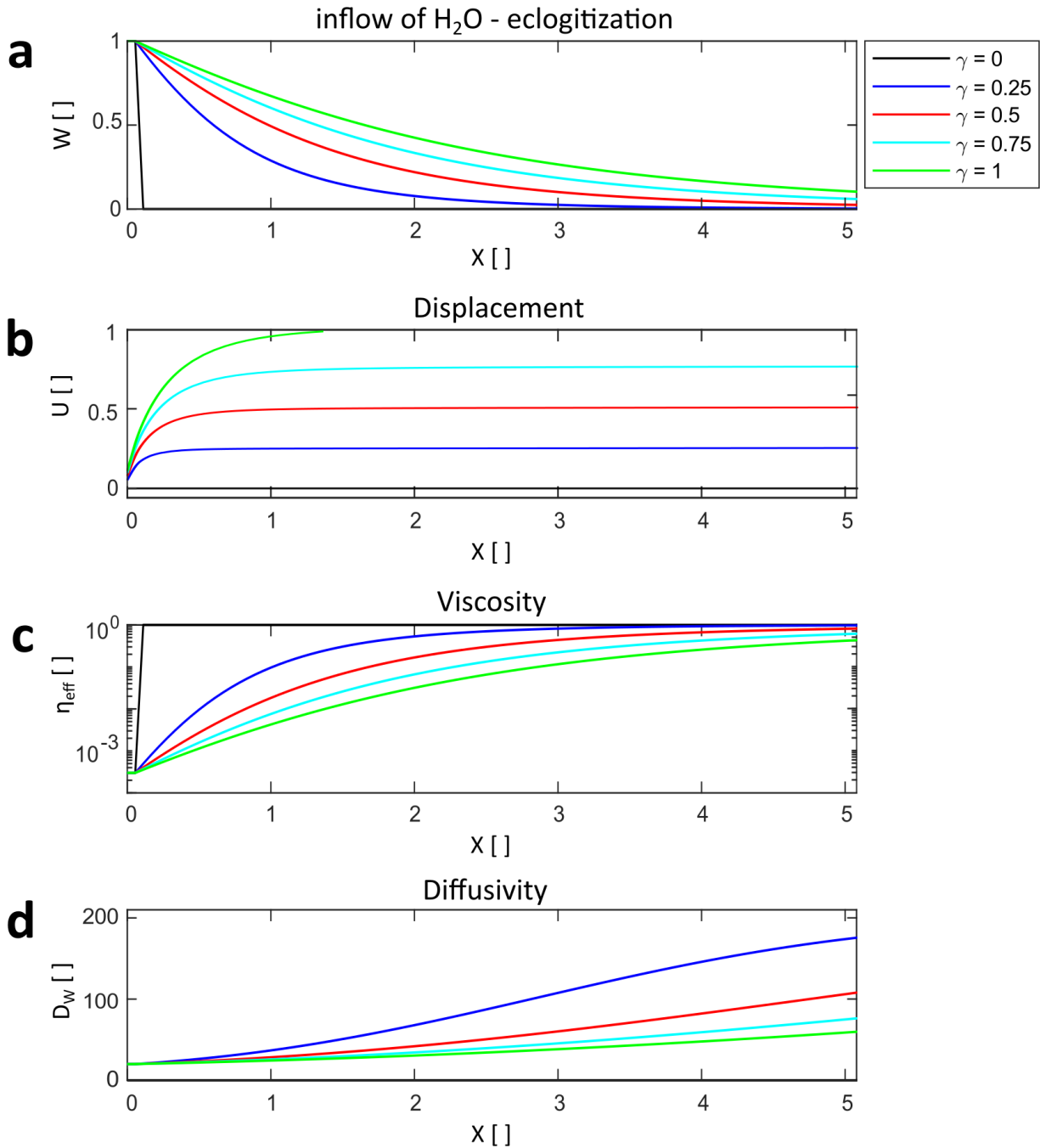
Figure 4.7. Lateral evolution of the non-linear H_2O inflow indicating the (a) eclogite-facies phase abundance W [ ] , (b) the normalized displacement adjusted by the shear zone width U [ ] , (c) the dimensionless effective viscosity η_{eff} [ ], and (d) the variable diffusivity D_W for five steps of shear strain from $\gamma = 0$ to $\gamma = 1$. X [ ] is the dimensionless distance divided by the shear zone width.

Systematics

More than 100 simulations were performed with various values for the dimensionless D_W (5 - 40) and the dimensionless $\eta 2$ ($10^{-5} - 10^{-2}$), to find the smallest misfit between normalized field-derived petrological and the modelled diffusion profiles (Figure 4.8). The petrological data values are

interpolated onto the grid points of the numerical model. Thereby the observed and modelled values for W and H can be compared at every numerical grid point. The relative difference between modelled and petrological value is calculated at every grid point and divided by the petrological value. The arithmetic average of all misfits along a profile, multiplied by 100, is then considered as average misfit in percent for each simulation. The misfit plot in Figure 4.8a shows that the required value of $\eta2$ to best fit the data increase with increasing values of D_W. Using a constant D_W, the minimum misfit reached is $< 9\%$ for $\eta2$ = 10^{-3}, and $D_W = 35$. As shown in Figure 4.8b the W-model profile does never perfectly fit the petrological profile (W-data).

To improve the fit that was obtained with constant D_W, more than 100 simulations with a variable D_W and variable $\eta2$ have been performed. Results show an almost perfect fit (Figure 4.8d) with values $a =$ 0.01 and $b = 0.5$ (see equation 4.V) with a minimum misfit $< 3\%$ (Figure 4.8c) at values of $\eta2 = 3*10^{-4}$ and $D_W = 20$. However, as described for Figure 4.7d the D_W decreased from granulite towards the shear zone, which is difficult to justify and discussed below.

Mechanical correction

Another possibility to fit the W-profile is to keep a constant D_W, but to assume that the shear zone also exhibited a component of shear zone-orthogonal flattening, that is a pure shear thinning component in addition to the simple shear component. A pure shear flattening component is frequently observed for natural shear zones. For example, Fossen and Cavalcante (2017) show that many natural shear zones feature a pure shear component (their figure 9). In case of a 1D simulation this causes a shortening of the material in x-direction. In the 1D shear zone model presented here, no simultaneous simple shearing and pure shear flattening can be simulated. Therefore, a pure shear shortening is applied to the final W-profile, which is obtained by simple shearing only. The main aim of applying such *a posteriori* pure shear flattening is to test whether such flattening could indeed decrease the misfit between the modelled and natural W-profiles.

The flattening is applied between coordinates 0 and 2 on the x-axis, to guarantee the conversion of natural observations that the pure shear flattening component is mainly present within and in close vicinity to the shear zone (Fossen and Cavalcante 2017). Results show that if a 30% flattening is applied, then it is possible to create an almost perfect fit (Figure 4.8d, yellow line). To find the best fit including pure shear flattening, results of the previous systematic simulations were used, and flattening was applied manually. The modelled and flattened profiles having the lowest percentage of flattening but the highest overlap with the W-profile, provide the following parameter: $\eta2 = 10^{-4}$, $D_W = 20$, and 30% flattening. These parameters are slightly different compared to Figure 4.8b.
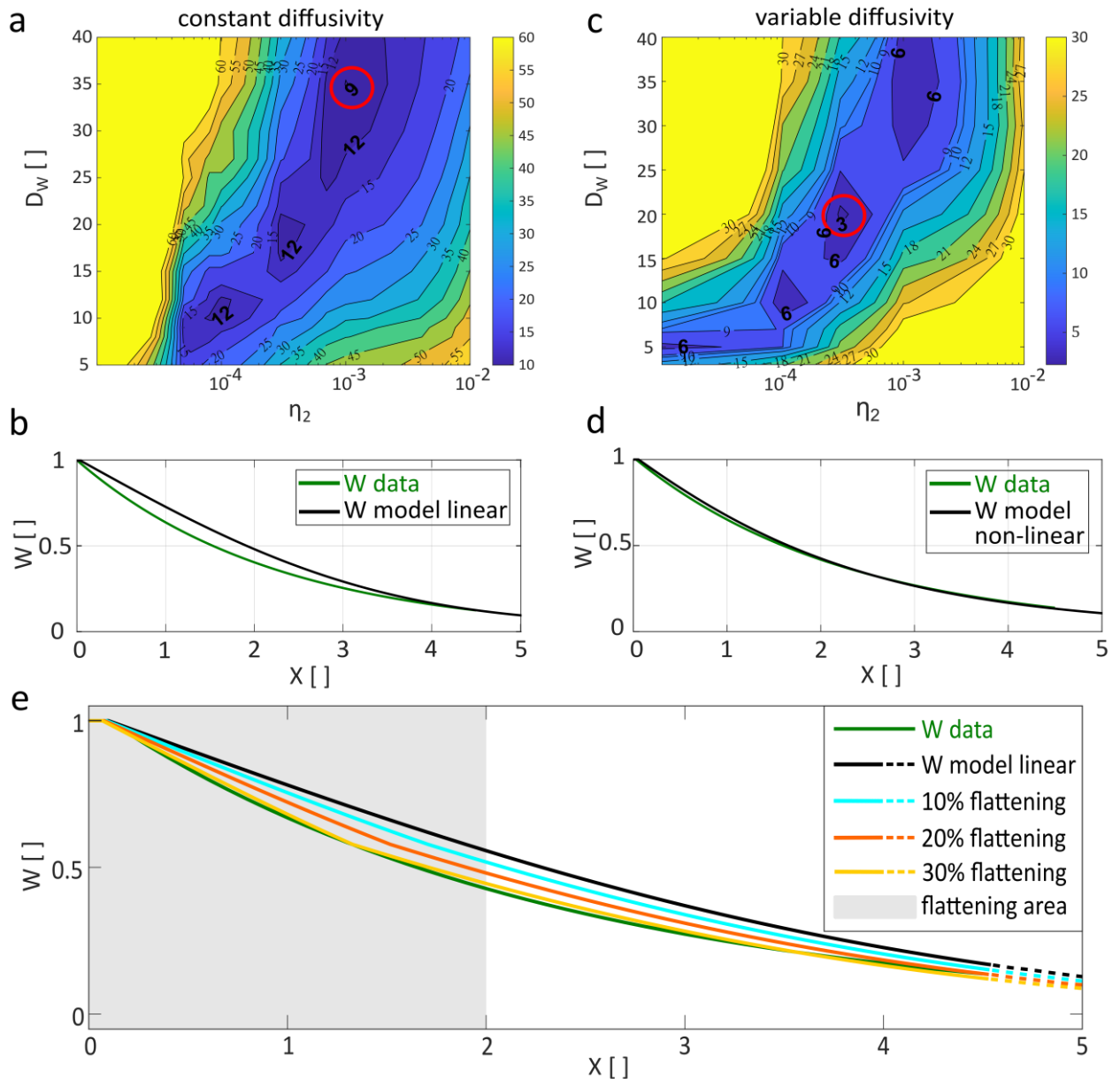
Figure 4.8. Best fit results of the inflow of H_2O, W, with constant diffusivity (a, b) and variable diffusivity (c, d). Contour-plots in (a) and (c) show various nondimensional diffusivities, D_W, vs. diverse nondimensional eclogite viscosities, $\eta 2$. The color bars display the misfit of the field-derived and the simulated W-profiles in %. The minimum misfit is 9% having a constant D_W and 3% with variable D_W. The related best fit profiles are displayed in (b) and (d) having the amount of W on the y-axis, where 1 response to 100% eclogite-facies phase, vs. the normalized distance, X, on the x-axis. (d) Results of linear inflow of H_2O including 10% - 30% pure shear flattening in the vicinity of the shear zone ($< 2 \, X \, [\,]$).

4.4.2 Double hydration: Fitting the inflow of H_2O (*W*) and hydrogen influx

(*H* – hydration of NAMs)

Constant D_W and D_H

In a second series of simulations, considering double hydration, the hydrogen influx is considered by including a second diffusion model into the shear zone model. The natural data indicate that the bulk hydrogen influx progressed further into the granulite (Figure 4.5d). To find the best fit diffusivity (D_H/D_W), and viscosity ratio ($\eta3/\eta2$) more than 100 simulations were performed. Both hydration processes were modelled with diffusion equations with constant D_W and D_H. Figure 4.9a shows the best fit results having an average misfit of ~ 4% for *W*, and ~ 10% for *H*, with $D_W = 19$, $D_H = \sim72$, which is ~3.8 times higher than D_W, $\eta2 = 10^{-4}$, and $\eta3 = 10^{-2}$. Best fit including flattening for both hydration processes between coordinates 0 and 2 on the x-axis (Figure 4.9b), resulting in: $D_W = 30$, $D_H = \sim124$ (4 times higher than D_W), $\eta2 = 10^{-4}$, $\eta3 = 10^{-2}$, and 30% flattening.
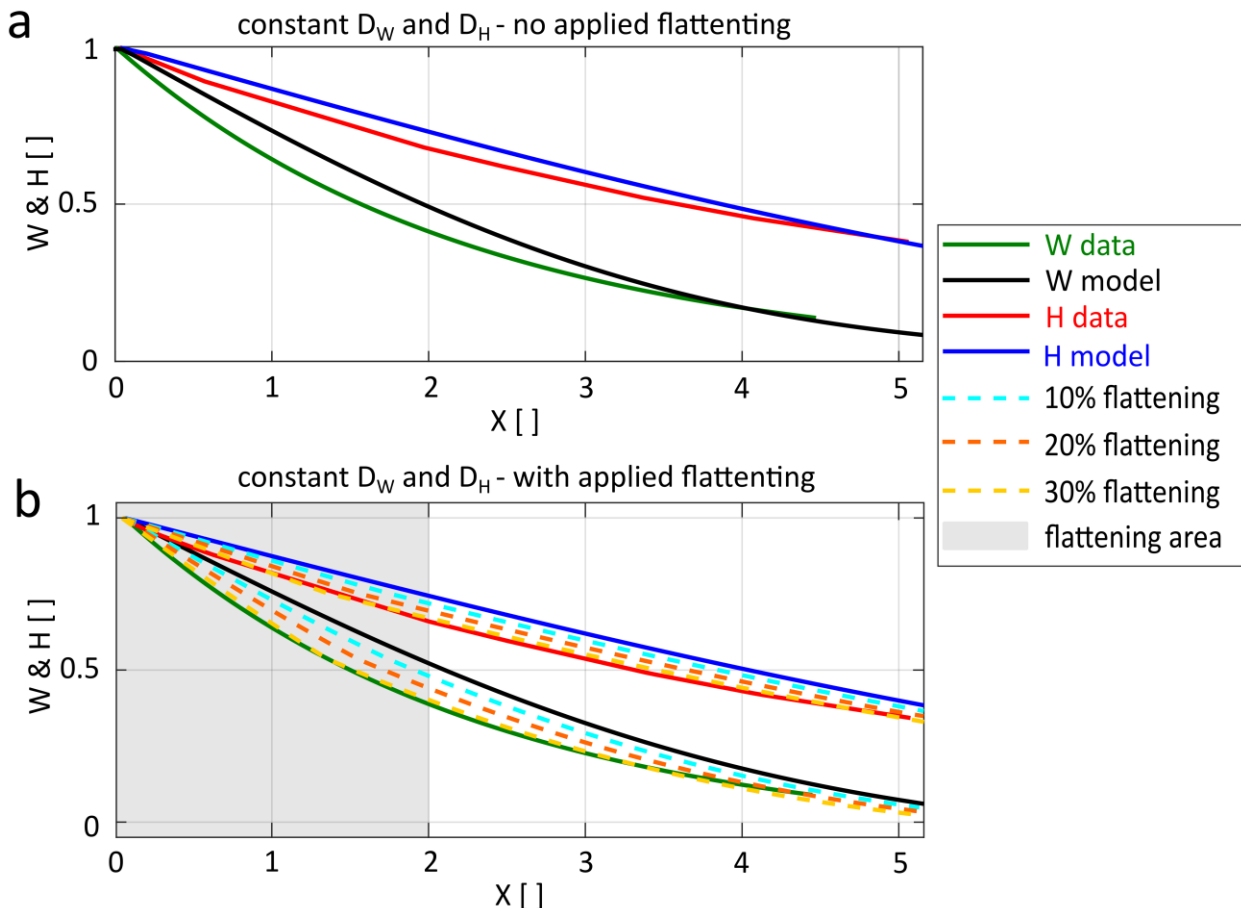
Figure 4.9. Double hydration due to H_2O inflow (W) and diffusional hydrogen influx (*H*) with constant D_W and D_H, respectively. Best fit results are given for (a) hydration profiles without flattening, and (b) with an applied flattening (10 – 30%). The amount of *W* and *H* are displayed on the y-axis, where 1 response to 100% eclogite-facies phase abundance for *W* and 100% water content in the NAMs for *H*. On the x-axis the nondimensional

distance, X [ ], is given. The lowest misfit is generated with a 30% flattening for $D_W = 30$, $D_H = \sim 124$, $\eta 2 = 10^{-4}$ and $\eta 3 = 10^{-2}$.

4.5 Discussion

The most striking result of this study is that diffusive hydrogen influx, in addition to aqueous fluid inflow, changes the ratio of total diffusivity to viscosity. Thereby, the petrologic data can be reproduced with a relatively simple 1D diffusion model.

4.5.1. Justification for the model set up

Field evidence and petrological data showed that the fluid influx, metamorphic reactions and deformation occurred contemporaneously, developing at different length and probable time scales (e.g., Kaatz et al. 2022). The shape of the averaged petrological profiles justifies the assumption that both hydration processes feature overall diffusion-type processes. Accordingly, both hydration processes, are approximated by and hence, modelled with a simple diffusion equation. The applied diffusion model, thus, does not model the exact hydration processes, but rather mimics all processes involved and resulted in the spatial and temporal variation of the H_2O inflow- and hydrogen influx profile (Figure 4.5d). During natural hydration, physical-chemical processes such as changing kinetics of mineral reactions, grain-size reduction, dissolution-transport-precipitation, mass-transfer or formation of transient porosity, and permeability occur and are certainly important. However, they are not explicitly considered in our model. The applied simple diffusion model represents an approximation of the combined effects of all such physical-chemical processes.

Local thermodynamic equilibrium

A recent study of Zertani et al. (2022) utilizes the static eclogite-facies overprint observed on Holsnøy to identify how hydration and eclogitization reactions are thermodynamically linked. They conclude that the reactive fluid flow, leading to eclogitization is guided by gains of the Gibbs free energy. Grain-boundaries with mineral reactions resulting in the highest energy drop occur first. This implies that the eclogitization far from equilibrium does not occur kinetically delayed (Zertani et al. 2022), and hence, the approximation of instantaneous mineral reactions is a valid assumption.

Diffusivity and porosity

The plg-plg reactions initiates a grain size minimization of the granulite matrix of about three orders of magnitude (Figure 4.3), accompanied by a densification and hence, local formation of porosity (e.g., Zertani et al. 2022). A transient porosity increase is a common feature of fluid-mediated rock transformation (e.g., Beinlich et al. 2020; John et al. 2012; Putnis 2021). Plümper et al. (2017) shows that the plg breakdown creates nanopores, which support electrokinetic fluid and mass transport through

the system without the need of an additional dynamic driving force such as high fluid pressure gradients. Additionally, Fusseis et al. (2009) suggests that within shear zones, fluids might be advectively transported via newly created pores during deformation-related dissolution-precipitation reactions, initiating a self-generated granular fluid pump. For the analyzed sample the determined remaining porosity after metamorphism and deformation shows a gradient in which the eclogite-facies shear zone has the highest with $1.8*10^{-2}$, the transition zone with $1.2*10^{-2}$ a moderate, and the original granulite with $5.5*10^{-3}$ the lowest porosity at 2.0 GPa (supplementary material ST4.4). It becomes evident that all observations and processes described above should result in an increase of the effective diffusivity of the infiltrating media from the granulite towards and into the shear zone. Contrary to this reasoning a decrease of the D_W and D_H has been found in the model with a variable diffusivity (Figure 4.7d). This is a counterintuitive behavior with respect to the measured porosity and the observed granulite to eclogite transformation. Consequently, the fitting applying a non-linear diffusivity, which creates increasing diffusivities from eclogite to granulite, is physically not feasible, although it produces a very good fit (Figure 4.8d).

Diffusivity and mechanical flattening

An additional mechanical correction was applied to the diffusion model. It is based on the findings of Fossen and Cavalcante (2017) that shear zones typically reveal a pure shear flattening of 10 - 40% within and in close vicinity to the shear zone. If this hold also true for the analyzed shear zone profile, the petrological data presented in Figure 4.5 already include a pure shear component, hence flattening of the initial rock. However, our most simple numerical model does only mimic the diffusional transport into the system during simple shear. Therefore, a pure shear component is applied during post processing within a restricted area from $0 - 2$ along the shear direction x (grey area Figure 4.9b). This is suitable for the investigated profiles because (1) bending of the granulite foliation is detectable throughout this area, and (2) granulitic plg grains already reacted leading to a very fine-grained matrix. These microstructures are probably related to a kind of ductile deformation. However, for the best fit, both final modelled hydration profiles do neither change the viscosity contrast (still $\eta 2 = 10^{-4}$, $\eta 3 = 10^{-2}$) nor the diffusivity ratio ($D_H = \sim 4 * D_W$) if flattening is applied.

4.5.2 Parametrization

The set of equations used in this study was solved in a non-dimensional form. To have an impression about the meaning of the outcome the strain rate $\dot{\varepsilon}$, shear stress τ, viscosities $\eta 1$-$\eta 3$, diffusivities D_W and D_H, and the duration t were recalculated assuming typical subduction zone velocities Vc. The recalculations are based on the best-fit results including a diffusional hydrogen influx and H_2O inflow with constant diffusivities, and 30% pure shear flattening as presented in Figure 4.9b, for a 2 cm wide shear zone. The shear zone width is in accordance with the analyzed shear zone profile. The simulations

show consistent results were (1) the viscosity ratio $\eta1/\eta2$ is 10^4, and 10^2 for $\eta1/\eta3$, and (2) $D_H/D_W = \sim$ 4. Figure 4.10 indicates a most likely range for all parameters.

Viscosities η1-η3

Previous studies use a minimum effective viscosity for the dry granulites on Holsnøy at given P-T-conditions of 10^{22} Pa.s (e.g., Bras et al. 2021; Labrousse et al. 2010), which is derived from an approximation for dry anorthite (e.g., Rybacki and Dresen 2000). Using the modelled viscosity ratios this results in a natural granulite viscosity of 10^{22} Pa.s, an effective eclogite viscosity of 10^{18} Pa.s, and an effective viscosity for the hydrated granulite of 10^{20} Pa.s during re-equilibration and shearing.

Contrary, to that outcome the findings of Hobbs et al. (2008) imply a viscosity contrast of one order of magnitude to be enough to guarantee ductile deformation (folding) of a single layer tested for dry albite vs. wet quartz by inferring a thermal-mechanical feedback. Schmid et al. (2010) commented that numerical simulations of a simple fold systems require viscosity contrasts of up to two orders of magnitude to allow for ductile deformation, which fits the results for $\eta3$. However, numerical simulations which are used to model ductile deformation of different materials are often based on experimentally-derived data resembling deformation processes and feedback-mechanisms of mono-mineralic materials at different P-T-conditions, time, and spatial scales as observed in natural rocks. Using field-based paleostress data of various mylonitic shear zones observed in lower crustal rocks Bürgmann and Dresen (2008) concluded that viscosity contrasts of up to three orders of magnitude between the rigid wall rock and weaker shear zone are required for ductile deformation by supposing constant far-field stress. These findings coincide with the field-based results presented here which are also in consistent with viscosity calculations of Bras et al. (2021).

Rheological behaviour

One of the outcomes is that the rheological behavior of the system changes when applying a diffusional hydrogen influx additional to the inflow of an aqueous fluid (Figure 4.8 vs. Figure 4.9). If only hydration by an aqueous fluid inflow is suggested viscosity ratio of $\eta1/\eta2$ (dry granulite/eclogite) is 10^3. Whereas the weakening effect is more enhanced if an additional influx by hydrogen is considered, $\eta1/\eta2 = 10^4$. This strongly suggests that hydrogen incorporation influences the effective viscosity of the affected rocks. It is well known that metamorphic re-equilibration by fluid-induced dissolution-precipitation processes and transient hydration of the wall rock often initiate significant rheological changes (e.g., Gueydan et al. 2003; Handy 1989; Plümper et al. 2017). Mechanisms such as dissolution-precipitation creep, dislocation creep, grain-boundary sliding, and diffusion creep facilitate to the transient weakening and increase the deformability of the system because they mainly control the evolution of the rock strength (e.g., Brodie and Rutter 1987; Marti et al. 2018; Oliot et al. 2010; Stünitz et al. 2020). Especially

plg, since it is the most abundant mineral occurring in the middle and upper crust, e.g., in the Holsnøy granulite it constitutes ~ 60 vol.%, plays a major role in the localized weakening and deformation (e.g., Altenberger and Wilhelm 2000; Wain et al. 2001; Wayte et al. 1989). The plg breakdown causes a reaction softening (e.g., Rubie 1983), which facilitates ductile deformation because recrystallized grain-sizes are reduced (e.g., Gerald and Stünitz 1993; Giuntoli et al. 2018; Tullis and Yund 1985; Wehrens et al. 2017). Nevertheless, it is still a matter of debate which mechanism actually weakens the plg, and if the incorporation of hydrogen already initiates a weakening. Potentially, the plg weakening is driven by dissolution-precipitation along the grain-boundaries as observed in qtz (e.g., Stünitz et al. 2017). Indeed, on Holsnøy, plg grain boundaries are highly reactive and the re-equilibrated mineral assemblage is very fine grained (Figure 4.3, e.g., Kaatz et al. 2022; Moore et al. 2019; Zertani et al. 2022). Additionally, Kaatz et al. (2022) demonstrate an immediate plg breakdown after limited hydrogen uptake, suggesting that the plg structure may become less stable after a certain level of OH-incorporation due to a pervasive hydrogen influx. Possibly, the plg weakening occurs similar to that of olivine, where hydrogen is bond to point defects within the crystal lattice, which promotes dislocation climb (e.g., Kohlstedt and Mackwell 1998; Mackwell et al. 1985; Mackwell and Kohlstedt 1990; Tielke et al. 2017). This progressively weakens the minerals over time. This may explain why the weakening affecting the rock seems to increase if a hydration due to a combination of aqueous fluid inflow and hydrogen influx is considered (see viscosity ratios above). Deciphering if hydrogen incorporation in plg is indeed contributing to the weakening should be part of upcoming research, since the significance of plg for deformation of the deep buried continental crust may still be underestimated.

Shear stress τ, Velocities Vc and Strain rate $\dot{\varepsilon}$

Figure 4.10 displays the shear stress (MPa) evolution for various $\eta2$, resulting in realistic range for $\eta1$ from $10^{21} - 10^{23}$ Pa.s, and values for *Vc* from $10^{-5} - 1$ cm/a. Most probable shear stresses (< 100 MPa) are generated if *Vc* is < 10^{-2} cm/a. The shear stress is based on the strain rate, $\dot{\varepsilon}$, which is a spatial derivative of *Vc*. If a *Vc* of > 10^{-2} cm/a is considered, the resulting $\dot{\varepsilon}$ are reaching values >10^{-10} s^{-1} that are rathe unlikely (Figure 4.10). The strain rate is not implemented into the numerical simulation as a references value but recalculated using the real shear zone width (in m) divided by the modelled shear zone width. Usually, strain rates used for similar shear zone models on Holsnøy are $10^{-14} - 10^{-13}$ s^{-1} (e.g., Bras et al. 2021; Kaatz et al. 2021; Labrousse et al. 2010). Lower limits of typical strain rates for crustal rocks and eclogite-facies shear bands are 10^{-14} s^{-1} (e.g., Fagereng and Biggs 2019), but can be as high as $10^{-13} - 10^{-12}$ s^{-1} (e.g., Terry and Heidelbach 2006), respectively. Convergence rates at subduction zones vary between approximately 2 – 10 cm/a (e.g., Syracuse et al. 2010), and are < 5 cm/a for continental collision zones (e.g., Guillot et al. 2003; Li 2014). Eclogitization and shear zone formation on Holsnøy occurs at > 80 km depth and include an entire network of single shear zones ranging from cm- to the km-scale, which are distributed over the entire region. Several authors show that strain is partitioned

within shear zones and especially, within large complex shear zone networks, which results in inhomogeneous deformation patterns (e.g., Carreras et al. 2013; Fossen and Cavalcante 2017; Fusseis et al. 2006; Schrank et al. 2008; Wehrens et al. 2017). Hence, a velocity partitioning among single shear zones of a contemporaneously active and evolving shear zone network, such as the one on Holsnøy, is supposed to result in low values of local Vc for the individual shear zones. Using typical strain rates ($10^{-14} - 10^{-13}$ s^{-1}), and shear zone widths (~ 0.5 m) as published in previous studies (e.g., Bras et al. 2021; Labrousse et al. 2010), calculated Vc vary between $10^{-5} - 10^{-4}$ cm/a, which is in agreement with the presented results.

Another remark is that the shear stresses increase linearly with increasing strain rates because of the linear viscous flow law used in the numerical model. If a power-law fluid flow would be applied, which is probably closer to reality but would result in more complexity, the stress increase would be less steep.

Diffusivities D_W, D_H

The diffusivity of the aqueous fluid inflow, D_W, and the hydrogen influx, D_H, are also given in Figure 4.10 for various $\eta 2$, different Vc, and for a 2 cm wide shear zone. If reasonable strain rates and shear stresses are applied ($Vc < 10^{-2}$ cm/a), D_W varies between $10^{-15} - 10^{-13}$ m^2/s, and D_H from $10^{-14} - 10^{-12}$ m^2/s. The difference between the two types of hydration are (1) volume diffusion through the crystal lattice accompanied by grain-boundary diffusion for the hydrogen influx, whereas (2) the aqueous fluid inflow, which delivers H_2O and additional hydrogen, is basically controlled by grain-boundary transport along already "hydrated" and equilibrating grain-boundaries (e.g., Kaatz et al. 2022). Referring to the diffusional hydrogen influx first, Ingrin and Blanchard (2006) demonstrate that reliable diffusivities for the hydrogen uptake in granulite- and eclogite-facies minerals such as grt and cpx vary between 10^{-15}, and 10^{-11} m^2/s for T > 900°C. Reynes et al. (2018) performed hydration experiments of grt at temperatures of 750°C and obtained diffusivities for hydrogen incorporation from $10^{-15} - 10^{-13}$ m^2/s. Additionally, the results of Dohmen and Milke (2010) imply bulk diffusion modelling including volume and grain-boundary diffusion and found an effective total diffusivity of 10^{-12} m^2/s. Consequentially, the modelled D_H value agrees with the current knowledge.

The modelled effective D_W is one order of magnitude lower than D_H. The resulting value of $10^{-14 \pm 1}$ m^2/s is in agreement with previously published bulk diffusivities for the infiltration of aqueous fluid on Holsnøy, when the applied strain rate is 10^{-13} s^{-1} (e.g., Bras et al. 2021; Kaatz et al. 2021; Malvoisin et al. 2020). However, inflow of aqueous fluid is controlled by grain-boundary diffusion, which is, especially under fluid saturated conditions and in reactive systems, very efficient with diffusivities of 10^{-12} m^2/s, (e.g., Dohmen and Milke 2010; Taetz et al. 2018). Dohmen and Milke (2010) conclude that typical diffusivity ratios of grain-boundary versus volume diffusion differ between $10^4 - 10^7$. This

suggests that the hydrogen influx is slowed down very significantly by its volume diffusion component, which results in rather similar bulk diffusivities of both hydration processes ($D_W = 10^{-14 \pm 1}$ m^2/s vs. $D_H = 10^{-13 \pm 1}$ m^2/s). Nevertheless, the D_H is only one order of magnitude faster compared to D_W, and both are in agreement with published values.

Time t, duration of the process

The duration calculated here is based on *Vc* and the shear zone width (2 cm). Time estimates for the duration of metamorphic rock transformation and single shear zone formation are rare, as it holds true for almost all rather short living geological processes (e.g., Beinlich et al. 2020). However, Kaatz et al. (2022) estimated a duration of 2 years for hydration of a single grt grain within the investigated shear zone within the scope of a previous study. This duration reflects the time the grt had to equilibrate with the elevated hydrogen concentration during the fluid-mediated shear zone formation. Using chronometric diffusion modeling, John et al. (2012), Taetz et al. (2018), and Beinlich et al. (2020) found lifetimes of metamorphic hydrothermal vein-wall rock systems to be ~800 a, ~20 a and a few months, respectively, with reaction front propagation velocities ranging between a few cm/a, and dm/a. Malvoisin et al. (2020) shows that fluid-induced densification reactions proceeds within the order of weeks. Furthermore, heat flow modelling using Ar^{40} – Ar^{39} mineral data indicate that a heating of a 30 m granulite lens from 385°C to 526°C (by ~700°C hot fluid) might have occurred within ~10 years (e.g., Camacho et al. 2005). According to these previous studies, it seems that a duration of less than 10 years for the eclogitization and deformation of the 2 cm wide shear zone studied here is rather unlikely. Hence, this is considered as another limiting factor for the recalculated results (Figure 4.10).
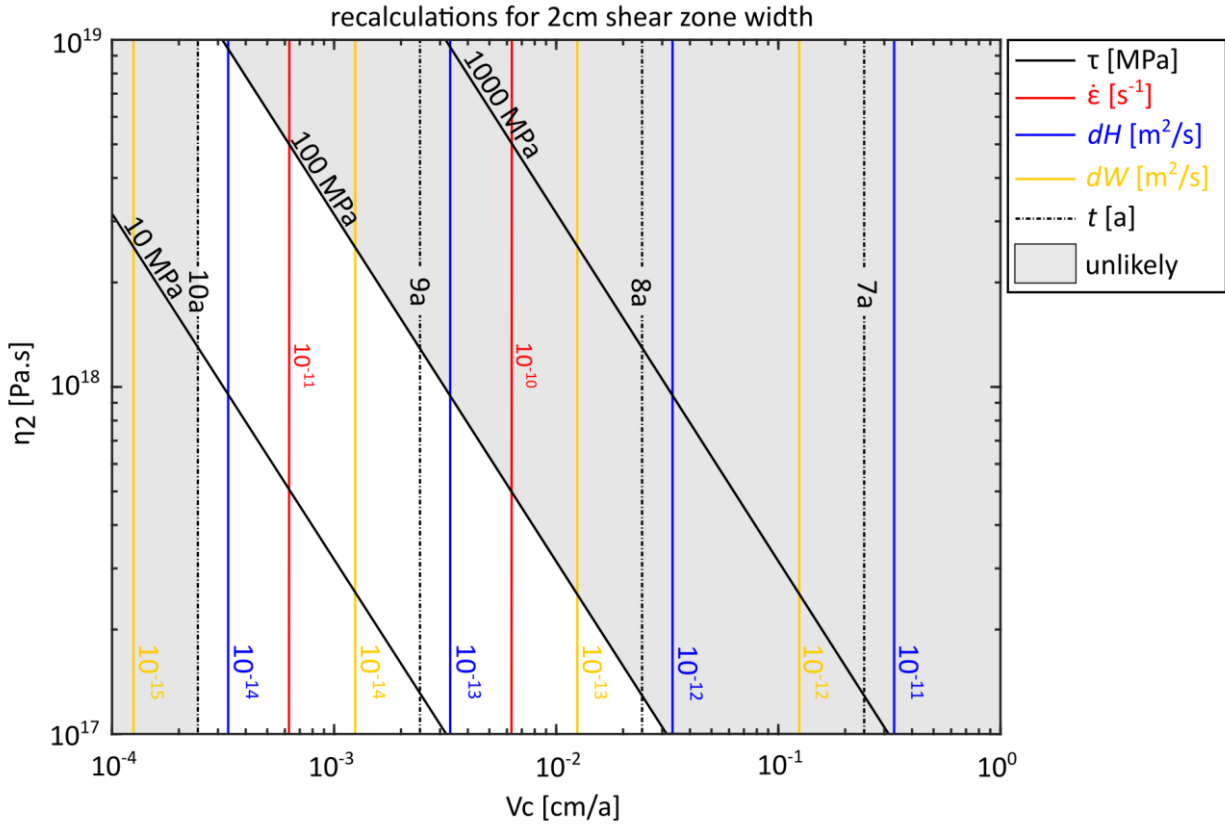
Figure 4.10. Recalculations of shear stress (τ), strain rate ($\dot{\varepsilon}$), hydrogen diffusivity (D_H), aqueous fluid diffusivity (D_W), and time (t) for various shear velocities (Vc), and eclogite viscosities ($\eta2$) of a 2 cm wide shear zone. Natural shear stresses of > 100 MPa and a time estimate > 10 years are unlikely, and consequently, build the limit of reliable associated parameters calculated here.

4.6 Conclusions

The presented results demonstrate that beside an inflow of aqueous fluid an additional hydrogen influx affects the evolving rock strength during fluid infiltration, metamorphic re-equilibration, and ductile deformation. Two contemporaneous but differently fast and pervasive hydration processes of H_2O and hydrogen were simulated using a simple 1D shear zone model. The results show that during equilibration and shearing the effective viscosity of the eclogite needs to be four orders of magnitudes lower than the one of the dry granulite. the effective viscosity of hydrated granulite needs to be two orders of magnitudes lower than the one of the dry granulite. Furthermore, the hydrogen influx slightly changes the effective diffusivities, where the diffusivity of hydrogen is approximately $10^{-14 \pm 1}$ m^2/s, and the aqueous fluid diffusivity $10^{-13 \pm 1}$ m^2/s. Estimates for the duration of the hydration and shearing, and constraints about the shear velocity are < 10 years and <10^{-2} cm.a^{-1}, respectively. This study shows how a simple numerical model, validated by constraints based on field data, can provide detailed information

on the dynamic evolution of petrophysical parameters of deeply buried crustal rocks. It describes how fluid inflow transiently modifies the rock strength of subducting continental crust.

4.7 Acknowledgments

The models used to produce the results presented in this study are given in the supplementary material of this dissertation (see file ST4.1).

References – Chapter 4

Altenberger U & Wilhelm S (2000) Ductile deformation of K-feldspar in dry eclogite facies s   hear zones in the Bergen Arcs, Norway. Tectonophysics, 320**,** 107-121.

Andersen TB, Corfu F, Labrousse L & Osmundsen P-T (2012) Evidence for hyperextension along the pre-Caledonian margin of Baltica. Journal of the Geological Society, 169**,** 601-612.

Andersen TB, Jamtveit B, Dewey JF & Swensson E (1991) Subduction and eduction of continental crust: major mechanisms during continent-continent collision and orogenic extensional collapse, a model based on the south Norwegian Caledonides. Terra Nova, 3**,** 303-310.

Austrheim H (1987) Eclogitization of lower crustal granulites by fluid migration through shear zones. Earth and Planetary Science Letters, 81**,** 221-232.

Austrheim H & Boundy TJS (1994) Pseudotachylytes generated during seismic faulting and eclogitization of the deep crust. 265**,** 82-83.

Austrheim H & Griffin WL (1985) Shear deformation and eclogite formation within granulite-facies anorthosites of the Bergen Arcs, western Norway. Chemical Geology, 50**,** 267-281.

Austrheim H & Robins B (1981) Reactions involving hydration of orthopyroxene in anorthosite-gabbro. Lithos, 14**,** 275-281.

Behrens H (2021) Hydrogen defects in feldspars: defect properties and implications for water solubility in feldspar. Physics and Chemistry of Minerals, 48**,** 1-22.

Beinlich A, John T, Vrijmoed JC, Tominaga M, Magna T & Podladchikov YY (2020) Instantaneous rock transformations in the deep crust driven by reactive fluid flow. Nature Geoscience, 13**,** 307-311.

Bhowany K, Hand M, Clark C, Kelsey D, Reddy S, Pearce M, Tucker N & Morrissey L (2018) Phase equilibria modelling constraints on P–T conditions during fluid catalysed conversion of granulite to eclogite in the Bergen Arcs, Norway. Journal of Metamorphic Geology, 36, 315-342. https://doi.org/10.1111/jmg.12294.

Boundy T, Fountain D & Austrheim H (1992) Structural development and petrofabrics of eclogite facies shear zones, Bergen Arcs, western Norway: implications for deep crustal deformational processes. Contributions to Mineralogy and Petrology, 10, 127-146.

Bras E, Baïsset M, Yamato P & Labrousse L (2021) Transient weakening during the granulite to eclogite transformation within hydrous shear zones (Holsnøy, Norway). Tectonophysics, 819, 229026.

Brodie K & Rutter E (1987) The role of transiently fine-grained reaction products in syntectonic metamorphism: natural and experimental examples. Canadian Journal of Earth Sciences, 24, 556-564.

Bürgmann R & Dresen G (2008) Rheology of the Lower Crust and Upper Mantle: Evidence from Rock Mechanics, Geodesy, and Field Observations. Annual Review of Earth and Planetary Sciences, 36, 531-567. 10.1146/annurev.earth.36.031207.124326.

Camacho A, Lee JK, Hensen BJ & Braun J (2005) Short-lived orogenic cycles and the eclogitization of cold crust by spasmodic hot fluids. Nature, 435, 1191-1196.

Carreras J, Cosgrove JW & Druguet E (2013) Strain partitioning in banded and/or anisotropic rocks: Implications for inferring tectonic regimes. Journal of Structural Geology, 50, 7-21.

Corfu F, Andersen TB & Gasser D (2014) The Scandinavian Caledonides: main features, conceptual advances and critical questions. Geological Society, London, Special Publications, 390, 9-43. http://dx.doi.org/10.1144/SP390.25.

De Ronde A, Stünitz H, Tullis J & Heilbronner R (2005) Reaction-induced weakening of plagioclase–olivine composites. Tectonophysics, 409, 85-106.

Deer WA, Howie RA & Zussman J. 1997. Rock-forming minerals: single-chain silicates, Volume 2A. Geological Society of London.

Dohmen R & Milke R (2010) Diffusion in polycrystalline materials: grain boundaries, mathematical models, and experimental data. Reviews in Mineralogy and Geochemistry, 72, 921-970. https://doi.org/10.2138/rmg.2010.72.21.

Fagereng Å & Biggs J (2019) New perspectives on 'geological strain rates' calculated from both naturally deformed and actively deforming rocks. Journal of Structural Geology, 125, 100-110.

Fossen H & Cavalcante GCG (2017) Shear zones–A review. Earth-Science Reviews, 171, 434-455.

Fossen H & Dunlap WJ (1998) Timing and kinematics of Caledonian thrusting and extensional collapse, southern Norway: evidence from 40Ar/39Ar thermochronology. Journal of structural geology, 20, 765-781. https://doi.org/10.1016/S0191-8141(98)00007-8.

Fountain DM, Boundy TM, Austrheim H & Rey P (1994) Eclogite-facies shear zones—deep crustal reflectors? Tectonophysics, 232, 411-424. https://doi.org/10.1016/0040-1951(94)90100-7.

Fusseis F, Handy MR & Schrank C (2006) Networking of shear zones at the brittle-to-viscous transition (Cap de Creus, NE Spain). Journal of Structural Geology, 28, 1228-1243. 10.1016/j.jsg.2006.03.022.

Fusseis F, Regenauer-Lieb K, Liu J, Hough R & De Carlo F (2009) Creep cavitation can establish a dynamic granular fluid pump in ductile shear zones. Nature, 459, 974-977.

Gerald JF & Stünitz H (1993) Deformation of granitoids at low metamorphic grade. I: Reactions and grain size reduction. Tectonophysics, 221, 269-297.

Gerya T. 2019. Introduction to numerical geodynamic modelling. Cambridge University Press.

Giuntoli F, Menegon L & Warren CJ (2018) Replacement reactions and deformation by dissolution and precipitation processes in amphibolites. Journal of Metamorphic Geology, 36, 1263-1286.

Glodny J, Kühn A & Austrheim H (2008) Geochronology of fluid-induced eclogite and amphibolite facies metamorphic reactions in a subduction–collision system, Bergen Arcs, Norway. Contributions to Mineralogy and Petrology, 156, 27-48. http://dx.doi.org/10.1007/s00410-007-0272-y.

Gueydan F, Leroy Y, Jolivet L & Agard P (2003) Analysis of continental localization induced by reaction-softening and microfracturing. Journal of Geophysical Research, 108.

Guillot S, Garzanti E, Baratoux D, Marquer D, Mahéo G & de Sigoyer J (2003) Reconstructing the total shortening history of the NW Himalaya. Geochemistry, Geophysics, Geosystems, 4.

Hacker BR, Andersen TB, Johnston S, Kylander-Clark AR, Peterman EM, Walsh EO & Young D (2010) High-temperature deformation during continental-margin subduction & exhumation: The ultrahigh-pressure Western Gneiss Region of Norway. Tectonophysics, 480, 149-171.

Halter WR, Macherel E & Schmalholz SM (2022) A simple computer program for calculating stress and strain rate in 2D viscous inclusion-matrix systems. Journal of Structural Geology, 160, 104617.

Handy MR (1989) Deformation regimes and the rheological evolution of fault zones in the lithosphere: the effects of pressure, temperature, grainsize and time. Tectonophysics, 163, 119-152.

Herwegh M, Berger A, Ebert A & Brodhag S (2008) Discrimination of annealed and dynamic fabrics: consequences for strain localization and deformation episodes of large-scale shear zones. Earth and planetary science letters, 276, 52-61.

Hobbs B, Regenauer-Lieb K & Ord A (2008) Folding with thermal–mechanical feedback. Journal of Structural Geology, 30, 1572-1592.

Incel S, Labrousse L, Hilairet N, John T, Gasc J, Shi F, Wang Y, Andersen TB, Renard F & Jamtveit B (2019) Reaction-induced embrittlement of the lower continental crust. Geology, 47, 235-238.

Ingrin J & Blanchard M (2006) Diffusion of hydrogen in minerals. Reviews in Mineralogy and Geochemistry, 62, 291-320.

Jackson JA, Austrheim H, McKenzie D & Priestley K (2004) Metastability, mechanical strength, and the support of mountain belts. Geology, 32. 10.1130/g20397.1.

Jakob J, Alsaif M, Corfu F & Andersen TB (2017) Age and origin of thin discontinuous gneiss sheets in the distal domain of the magma-poor hyperextended pre-Caledonian margin of Baltica, southern Norway. Journal of the Geological Society, 174, 557-571. https://doi.org/10.1144/jgs2016-049.

Jamtveit B, Ben-Zion Y, Renard F & Austrheim H (2018a) Earthquake-induced transformation of the lower crust. Nature, 556, 487-491. https://doi.org/10.1029/2018JB016461.

Jamtveit B, Bucher-Nurminen K & Austrheim H (1990) Fluid controlled eclogitization of granulites in deep crustal shear zones, Bergen arcs, Western Norway. Contributions to Mineralogy Petrology, 104, 184-193.

Jamtveit B, Dunkel KG, Petley-Ragan A, Austrheim H, Corfu F & Schmid DW (2021) Rapid fluid-driven transformation of lower continental crust associated with thrust-induced shear heating. Lithos, 396, 106216.

Jamtveit B, Moulas E, Andersen TB, Austrheim H, Corfu F, Petley-Ragan A & Schmalholz SM (2018b) High Pressure Metamorphism Caused by Fluid Induced Weakening of Deep Continental Crust. Scientific reports, 8, 17011. https://doi.org/10.1038/s41598-018-35200-1.

Jamtveit B, Petley-Ragan A, Incel S, Dunkel KG, Aupart C, Austrheim H, Corfu F, Menegon L & Renard F (2019) The effects of earthquakes and fluids on the metamorphism of the lower continental crust. Journal of Geophysical Research: Solid Earth, 124, 7725-7755. https://doi.org/10.1029/2018JB016461.

John T, Gussone N, Podladchikov YY, Bebout GE, Dohmen R, Halama R, Klemd R, Magna T & Seitz H-M (2012) Volcanic arcs fed by rapid pulsed fluid flow through subducting slabs. Nature Geoscience, 5, 489-492.

John T & Schenk V (2003) Partial eclogitisation of gabbroic rocks in a late Precambrian subduction zone (Zambia): prograde metamorphism triggered by fluid infiltration. Contributions to Mineralogy and Petrology, 146, 174-191. https://doi.org/10.1007/s00410-003-0492-8.

Jolivet L, Raimbourg H, Labrousse L, Avigad D, Leroy Y, Austrheim H & Andersen TB (2005) Softening trigerred by eclogitization, the first step toward exhumation during continental subduction. Earth and Planetary Science Letters, 237, 532-547. https://doi.org/10.1016/j.epsl.2005.06.047.

Kaatz L, Reynes J, Hermann J & John T (2022) How fluid infiltrates dry crustal rocks during progressive eclogitization and shear zone formation: insights from H2O contents in nominally anhydrous minerals. Contributions to Mineralogy and Petrology, 177, 1-20.

Kaatz L, Zertani S, Moulas E, John T, Labrousse L, Schmalholz SM & Andersen TB (2021) Widening of hydrous shear zones during incipient eclogitization of metastable dry and rigid lower crust—Holsnøy, western Norway. Tectonics, 40. https://doi.org/10.1029/2020TC006572.

Katayama I & Karato S-I (2008) Effects of water and iron content on the rheological contrast between garnet and olivine. Physics of the Earth and Planetary Interiors, 166, 57-66. https://doi.org/10.1016/j.pepi.2007.10.004.

Klemd R, John T, Scherer EE, Rondenay S & Gao J (2011) Changes in dip of subducted slabs at depth: Petrological and geochronological evidence from HP–UHP rocks (Tianshan, NW-China). Earth and Planetary Science Letters, 310, 9-20. 10.1016/j.epsl.2011.07.022.

Kohlstedt DL & Mackwell SJ (1998) Diffusion of hydrogen and intrinsic point defects in olivine. Zeitschrift für physikalische Chemie, 207, 147-162.

Labrousse L, Hetényi G, Raimbourg H, Jolivet L & Andersen TB (2010) Initiation of crustal-scale thrusts triggered by metamorphic reactions at depth: Insights from a comparison between the Himalayas and Scandinavian Caledonides. Tectonics, 29, n/a-n/a. 10.1029/2009tc002602.

Lasaga A. 1998. Kinetic theory in the earth sciences. 1998. Princeton university press.

Li Z (2014) A review on the numerical geodynamic modeling of continental subduction, collision and exhumation. Science China Earth Sciences, 57, 47-69.

Llana-Fúnez S, Wheeler J & Faulkner DR (2012) Metamorphic reaction rate controlled by fluid pressure not confining pressure: implications of dehydration experiments with gypsum. Contributions to Mineralogy and Petrology, 164, 69-79.

Mackwell S, Bai Q & Kohlstedt D (1990) Rheology of olivine and the strength of the lithosphere. Geophysical Research Letters, 17, 9-12.

Mackwell S, Kohlstedt D & Paterson M (1985) The role of water in the deformation of olivine single crystals. Journal of Geophysical Research: Solid Earth, 90, 11319-11333.

Mackwell SJ & Kohlstedt DL (1990) Diffusion of hydrogen in olivine: implications for water in the mantle. Journal of Geophysical Research: Solid Earth, 95, 5079-5088.

Malvoisin B, Austrheim H, Hetényi G, Reynes J, Hermann J, Baumgartner LP & Podladchikov YY (2020) Sustainable densification of the deep crust. Geology, 48(7), 673-677.

Malvoisin B, Podladchikov YY & Vrijmoed JC (2015) Coupling changes in densities and porosity to fluid pressure variations in reactive porous fluid flow: Local thermodynamic equilibrium. Geochemistry, Geophysics, Geosystems, 16, 4362-4387.

Mancktelow NS & Pennacchioni G (2005) The control of precursor brittle fracture and fluid–rock interaction on the development of single and paired ductile shear zones. Journal of Structural Geology, 27, 645-661. 10.1016/j.jsg.2004.12.001.

Manning CE (2004) The chemistry of subduction-zone fluids. Earth and Planetary Science Letters, 223, 1-16. https://doi.org/10.1016/j.epsl.2004.04.030.

Manning CE & Frezzotti ML (2020) Subduction-zone fluids. Elements: An International Magazine of Mineralogy, Geochemistry, and Petrology, 16**,** 395-400. https://doi.org/10.2138/gselements.16.6.395.

Marti S, Stünitz H, Heilbronner R, Plümper O & Kilian R (2018) Syn-kinematic hydration reactions, grain size reduction, and dissolution–precipitation creep in experimentally deformed plagioclase–pyroxene mixtures. Solid Earth, 9**,** 985-1009.

Mattey D, Jackson D, Harris N & Kelley S (1994) Isotopic constraints on fluid infiltration from an eclogite facies shear zone, Holsenøy, Norway. Journal of Metamorphic Geology, 12**,** 311-325.

Menegon L, Pennacchioni G, Malaspina N, Harris K & Wood E (2017) Earthquakes as precursors of ductile shear zones in the dry and strong lower crust. Geochemistry, Geophysics, Geosystems, 18**,** 4356-4374.

Moore J, Beinlich A, Austrheim H & Putnis A (2019) Stress orientation–dependent reactions during metamorphism. Geology, 47**,** 151-154.

Mosenfelder JL, Rossman GR & Johnson EA (2015) Hydrous species in feldspars: A reassessment based on FTIR and SIMS. American Mineralogist, 100**,** 1209-1221.

Moulas E, Kaus B & Jamtveit B (2022) Dynamic pressure variations in the lower crust caused by localized fluid-induced weakening. Communications Earth & Environment, 3.

Mukai H, Austrheim H, Putnis CV & Putnis A (2014) Textural evolution of plagioclase feldspar across a shear zone: implications for deformation mechanism and rock strength. Journal of Petrology, 55**,** 1457-1477.

Oliot E, Goncalves P & Marquer D (2010) Role of plagioclase and reaction softening in a metagranite shear zone at mid-crustal conditions (Gotthard Massif, Swiss Central Alps). Journal of Metamorphic Geology, 28**,** 849-871.

Padrón-Navarta JA, Hermann J & O'Neill HSC (2014) Site-specific hydrogen diffusion rates in forsterite. Earth and Planetary Science Letters, 392**,** 100-112. https://doi.org/10.1016/j.epsl.2014.01.055.

Pennacchioni G & Mancktelow NS (2007) Nucleation and initial growth of a shear zone network within compositionally and structurally heterogeneous granitoids under amphibolite facies conditions. Journal of Structural Geology, 29**,** 1757-1780.

Petley-Ragan A, Dunkel KG, Austrheim H, Ildefonse B & Jamtveit B (2018) Microstructural records of earthquakes in the lower crust and associated fluid-driven metamorphism in plagioclase-rich granulites. Journal of Geophysical Research: Solid Earth, 123**,** 3729-3746. https://doi.org/10.1029/2017JB015348.

Piccoli F, Hermann J, Pettke T, Connolly J, Kempf ED & Duarte JV (2019) Subducting serpentinites release reduced, not oxidized, aqueous fluids. Scientific reports, 9**,** 1-7.

Plümper O, Botan A, Los C, Liu Y, Malthe-Sørenssen A & Jamtveit B (2017) Fluid-driven metamorphism of the continental crust governed by nanoscale fluid flow. Nature geoscience, 10, 685-690.

Pollard D & Fletcher RC. 2005. Fundamentals of structural geology. Cambridge University Press.

Pollok K, Lloyd GE, Austrheim H & Putnis A (2008) Complex replacement patterns in garnets from Bergen Arcs eclogites: A combined EBSD and analytical TEM study. Chemie der Erde - Geochemistry, 68, 177-191. 10.1016/j.chemer.2007.12.002.

Putnis A (2021) Fluid–Mineral Interactions: Controlling Coupled Mechanisms of Reaction, Mass Transfer and Deformation. Journal of Petrology, 62, egab092.

Putnis A & Austrheim H (2010) Fluid-induced processes: metasomatism and metamorphism. Geofluids. https://doi.org/10.1111/j.1468-8123.2010.00285.x.

Putnis A & John T (2010) Replacement processes in the Earth's crust. Elements, 6, 159-164. https://doi.org/10.2113/gselements.6.3.159.

Raimbourg H, Goffé B & Jolivet L (2007a) Garnet reequilibration and growth in the eclogite facies and geodynamical evolution near peak metamorphic conditions. Contributions to Mineralogy and Petrology, 153, 1-28. 10.1007/s00410-006-0130-3.

Raimbourg H, Jolivet L, Labrousse L, Leroy Y & Avigad D (2005) Kinematics of syneclogite deformation in the Bergen Arcs, Norway: implications for exhumation mechanisms. Geological Society, London, Special Publications, 243, 175-192. https://doi.org/10.1144/GSL.SP.2005.243.01.13.

Raimbourg H, Jolivet L & Leroy Y (2007b) Consequences of progressive eclogitization on crustal exhumation, a mechanical study. Geophysical Journal International, 168, 379-401. 10.1111/j.1365-246X.2006.03130.x.

Reynes J, Jollands M, Hermann J & Ireland T (2018) Experimental constraints on hydrogen diffusion in garnet. Contributions to mineralogy and petrology, 173, 69. https://doi.org/10.1007/s00410-018-1492-z.

Roberts D (2003) The Scandinavian Caledonides: event chronology, palaeogeographic settings and likely modern analogues. Tectonophysics, 365, 283-299. https://doi.org/10.1016/S0040-1951(03)00026-X.

Rubie DC (1983) Reaction-enhanced ductility: The role of solid-solid univariant reactions in deformation of the crust and mantle. Tectonophysics, 96, 331-352.

Rybacki E & Dresen G (2000) Dislocation and diffusion creep of synthetic anorthite aggregates. Journal of Geophysical Research: Solid Earth, 105, 26017-26036.

--- (2004) Deformation mechanism maps for feldspar rocks. Tectonophysics, 382, 173-187.

Schmid DW, Schmalholz SM, Mancktelow NS & Fletcher RC (2010) Comment on 'Folding with thermal-mechanical feedback'. Journal of Structural Geology, 32**,** 127 - 130. 0.1016/j.jsg.2009.10.004.

Schneider F, Yuan X, Schurr B, Mechie J, Sippl C, Haberland C, Minaev V, Oimahmadov I, Gadoev M & Radjabov N (2013) Seismic imaging of subducting continental lower crust beneath the Pamir. Earth and Planetary Science Letters, 375**,** 101-112.

Schrank C, Handy M & Fusseis F (2008) Multiscaling of shear zones and the evolution of the brittle-to-viscous transition in continental crust. Journal of Geophysical Research: Solid Earth, 113.

Stalder R, Purwin H & Skogby H (2007) Influence of Fe on hydrogen diffusivity in orthopyroxene. European Journal of Mineralogy, 19**,** 899-903. https://doi.org/10.1127/0935-1221/2007/0019-1780.

Stünitz H, Neufeld K, Heilbronner R, Finstad AK, Konopásek J & Mackenzie JR (2020) Transformation weakening: diffusion creep in eclogites as a result of interaction of mineral reactions and deformation. Journal of Structural Geology, 139**,** 104129.

Stünitz H, Thust A, Heilbronner R, Behrens H, Kilian R, Tarantola A & Fitz Gerald J (2017) Water redistribution in experimentally deformed natural milky quartz single crystals—Implications for H_2O-weakening processes. Journal of Geophysical Research: Solid Earth, 122**,** 866-894.

Syracuse EM, van Keken PE & Abers GA (2010) The global range of subduction zone thermal models. Physics of the Earth and Planetary Interiors, 183**,** 73-90.

Taetz S, John T, Bröcker M, Spandler C & Stracke A (2018) Fast intraslab fluid-flow events linked to pulses of high pore fluid pressure at the subducted plate interface. Earth and Planetary Science Letters, 482**,** 33-43.

Terry MP & Heidelbach F (2006) Deformation-enhanced metamorphic reactions and the rheology of high-pressure shear zones, Western Gneiss Region, Norway. Journal of Metamorphic Geology, 24**,** 3-18. 10.1111/j.1525-1314.2005.00618.x.

Tielke JA, Zimmerman ME & Kohlstedt DL (2017) Hydrolytic weakening in olivine single crystals. Journal of Geophysical Research: Solid Earth, 122**,** 3465-3479.

Tollan P & Hermann J (2019) Arc magmas oxidized by water dissociation and hydrogen incorporation in orthopyroxene. Nature geoscience, 12**,** 667-671.

Tollan PM, O'Neill HSC & Hermann J (2018) The role of trace elements in controlling H incorporation in San Carlos olivine. Contributions to Mineralogy and Petrology, 173**,** 1-23.

Tullis J & Yund RA (1985) Dynamic recrystallization of feldspar: A mechanism for ductile shear zone formation. Geology, 13**,** 238-241. https://doi.org/10.1130/0091-7613(1985)13%3C238:DROFAM%3E2.0.CO;2.

Turcotte DL & Schubert G. 2014. Geodynamics. Cambridge University Press, Cambridge.

Wain A, Waters D & Austrheim H (2001) Metastability of granulites and processes of eclogitisation in the UHP region of western Norway. Journal of Metamorphic Geology, 19, 609-625.

Wayte GJ, Worden RH, Rubie DC & Droop GT (1989) A TEM study of disequilibrium plagioclase breakdown at high pressure: the role of infiltrating fluid. Contributions to Mineralogy and Petrology, 101, 426-437.

Wehrens P, Baumberger R, Berger A & Herwegh M (2017) How is strain localized in a meta-granitoid, mid-crustal basement section? Spatial distribution of deformation in the central Aar massif (Switzerland). Journal of structural geology, 94, 47-67.

Yuan X, Sobolev SV, Kind R, Oncken O, Bock G, Asch G, Schurr B, Graeber F, Rudloff A & Hanka WJN (2000) Subduction and collision processes in the Central Andes constrained by converted seismic phases. 408, 958.

Zertani S, John T, Brachmann C, Vrijmoed JC & Plümper O (2022) Reactive fluid flow guided by grain-scale equilibrium reactions during eclogitization of dry crustal rocks. Contributions to Mineralogy and Petrology, 177, 1-18.

Zertani S, Labrousse L, John T, Andersen TB & Tilmann F (2019) The interplay of Eclogitization and deformation during deep burial of the lower continental crust—A case study from the Bergen Arcs (Western Norway). Tectonics, 38, 898-915.

Zheng Y-F & Hermann J (2014) Geochemistry of continental subduction-zone fluids. Earth, Planets and Space, 66, 1-16.

Chapter 5

Conclusions and Outlook

5.1 Conclusions

The subduction of continental crust still is an enigmatic phenomenon of the Earth's recycling process and has been part of ongoing research for decades. It is not possible to investigate the ongoing processes in detail while they occur especially, when occurring at HP-HT-conditions. Classical petrological and structural investigations are indispensable to get a comprehensive picture of the processes, arising at great depth. But these investigations are only possible if the material is exhumed and exposed at the Earth's surface. The information about mineral assemblages, structures within various scales, and element composition help to interpret data derived from, e.g., receiver-function imaging, as well as provide data to perform numerical simulations. This interplay of interdisciplinary methods successively contributes new knowledge to unravel mysteries like the deep subduction of highly buoyant continental crust.

This thesis presents research, bridging detailed field mapping, petrological high-resolution analyses (FTIR, EMPA), and conservative numerical simulation using field-derived data. Thereby, the results aim to contribute to the question of how continental crust transforms during deep burial as a consequence of brittle and ductile deformation accompanied by fluid-rock interaction. Granulites exposed on Holsnøy have been partially eclogitized due to the infiltration of an external fluid. The eclogitization either occurred by static eclogite-facies overprint without any associated deformation or by simultaneous ductile deformation, causing eclogite-facies shear zone formation. Networking of single shear zones and progressive widening lead to the development of a km-scale shear zone network. Within the scope of this study, it was possible to reveal that a substantial amount of fluid was necessary to guarantee the shear zone evolution as exposed. Detailed field mapping of two outcrops was the basis for numerical simulations, which reproduce similar first order shear zone geometries during shearing and fluid infiltration into low viscosity zones. These new results do not only provide the necessity of a significant fluid amount, either introduced by numerous repetitive single pulses or by one substantial event, but additionally imply that (1) the fluid influx forms a hydration halo parallel to the shear zone boundaries, which causes a viscosity gradient between rigid granulite and temporarily weaker eclogite; (2) the calculated effected diffusivity of the bulk fluid diffusion is approximately $D_b = 10^{-16 \pm 1}$ m^2/s; and (3) the orientation of the shear zones, with respect to the far-field stress, influences the evolution of the dynamic pressure and stress. Changing pressures during shearing and rotation (bookshelf-type deformation) indicate that the shear zones first absorb the fluid and then expel it either towards the wall rock or along the shear zone network. Based on these results, new open questions have been raised. How does the fluid influx proceed and how far does hydration propagate into the granulite? Is it possible to estimate natural pressures, stresses, and viscosities during shear zone formation and hydration?

One eclogite-facies shear zone profile was investigated in detail and thus, aid addressing these issues. To quantify the hydration, especially at an early stage, it was necessary to analyze a cm-scale eclogite-facies shear zone at incipient eclogitization to ensure that hydration along the pre-cursor fracture just started. Furthermore, amphibolite-facies overprint needs to be excluded because it would have partially rehydrated the system, reactivated the present structures, and transformed the mineral assemblage by retrogression. Hence, amphibolite-facies overprint would eliminate any reliable subsequent investigations to explain the prograde hydration of the granulite. Microscopic analysis revealed one sample to be suitable for further investigations of the NAMs constituting the granulite.

Using FTIR-derived water content profiles, comprehensive EMPA measurements, and SEM analysis, it was possible to prove that the hydration occurred in two contemporaneous fluid influxes causing different mechanisms to act simultaneously at different spatial and time scales. This finding was recorded in the NAMs indicating a pervasive hydrogen influx. This diffusional hydrogen influx was driven by grain-boundary and volume diffusion, decorates pre-existing defects within the crystal lattice of single grains, and progressed further into the granulite. It causes no compositional changes but the incorporation of hydrogen bond to the oxygen in the crystal lattice leads to a measurable OH-increase within the grain interiors from ~ 10 to ~ 50 µg/g for grt, ~ 50 to ~ 310 µg/g for cpx, and ~ 10 to ~ 140 µg/g for plg. A simultaneous inflow of aqueous fluid enables element transfer along the grain-boundaries causing extensive eclogite-facies re-equilibration reactions. These are recorded by the formation of eclogite-facies phases as well as by reaction rims of different composition holding increased water contents. The petrological dataset was utilized to perform numerical simulations, which reveal that the diffusional hydrogen influx is one order of magnitude faster ($D_H = 10^{-13 \pm 1}$ m^2/s) compared to the inflow of an aqueous fluid ($D_W = 10^{-14 \pm 1}$ m^2/s). Strikingly, D_W is consistent with D_b for bulk diffusion as provided above (no. 2). However, the granulite hydration is indeed not limited to the eclogite-facies shear zones. Hydrogen is pervasively transported into the granulite grains, and possibly initiates a first weakening of the metastable and rigid system, which may explain the detected gradual viscosity ratio between granulite and eclogite (no. 1 above).

The same numerical simulations reveal that the rheology of the system was affected by both hydrogen influx, and inflow of an aqueous fluid. The viscosity of the hydrated granulite (through hydrogen influx) must have been at least two orders of magnitude lower compared to the dry granulite, whereas the re-equilibrating eclogite must have been four orders of magnitude weaker (through aqueous fluid inflow) to replicate the shear zone geometry as observed on Holsnøy. If only an aqueous fluid inflow is suggested, viscosity contrast between granulite and re-equilibrating eclogite is one order of magnitude less, as observed when both hydration processes are modelled. This rheological effect is probably driven by plg, which constitutes approximately 60 vol.% of the granulite. The results presented in this work

prove that the plg breaks down after limited hydrogen incorporation, where no eclogite-facies phases are abundant, and cause a huge grain size minimization of the granulite matrix. This triggers and promotes a wide variety of interdependent processes, e.g., creep mechanisms facilitating to the progressive weakening. However, if hydrogen incorporation in plg already weakens the system or which mechanisms are involved, is still a matter of debate. But the results presented in this work provide new insights about the crucial effect of hydrogen influx on the weakening of a dry crustal rock.

Furthermore, recalculations of the results of the numerical simulation to natural conditions indicate that the granulite hydration and cm-scale eclogite-facies shear zone formation probably takes less than ten years at local shear velocities less than 10^{-2} cm/a. Compared to subduction zone velocities these velocities are very slow and hence, imply velocity partitioning. Strain partitioning in highly complex geometries enables considerable inhomogeneities in stress, pressures and temperature. Therefore, it should be part of the upcoming research to unravel distribution of velocity variations within such geometries.

To conclude, the results of this study explicitly highlight the role of fluid- and especially hydrogen-induced weakening and re-equilibration of subducted metastable dry crustal rocks. Furthermore, it was demonstrated how detailed field observation and rock sample analyses can be used to provide not only information about mineralogy, microstructures or composition, but also to extract natural estimates about shear stress, strain rates, diffusivities, and duration of several processes using a simple 1D numerical simulation. Approaches like that can contribute significantly to our knowledge of crustal weakening.

5.2 Outlook

The results of this study emphasize that hydration of a dry crustal rock by an external fluid, mainly composed of H_2O, is not only driven by the recrystallization of hydrous minerals due to fluid-rock interaction but as well by the acceptance of NAMs to incorporate and store large amounts of OH-groups in their crystal lattice. However, these minerals are typically considered to be "dry". This work underlines that especially plg plays a major role in the weakening of subducting continental crust. Plagioclase constitutes large volumes of the continental crust and is the first phase to break down at high P-conditions, causing a substantial decrease in the average matrix grain-size of the system. Strikingly, the presented results show that the plg breakdown occurs in close vicinity but also further away from shear zones possibly caused by the pervasive transport of hydrogen. Therefore, a comprehensive approach would be necessary to identify if hydrogen incorporation initiates a weakening, e.g., like observed in olivine, where hydrogen bonded to pre-existing point defects initiates climb mechanisms, which subsequently weaken the material. To do so, knowledge about the oxygen fugacity within the

eclogite-facies shear zones and the granulite would be important because it highly affects the hydrogen weakening of other phases. Furthermore, oxygen fugacity data would help to enable a hydrogen specification, whether the aqueous fluid rather provides H_2 or H^+.

Additionally, the presented numerical simulations provide new time estimates of less than ten years for shear zone formation, eclogitization and hydration on cm-scales. However, accurate estimates about reaction front propagation would enable a clear insight into how long eclogitization processes may last. Using Lithium-isotopes short-lived hydration events can be analyzed. Hence, these results may provide time estimates as well as further conclusions about the diffusivity of the fluid.

Besides, parts of the presented results are based on one single shear zone profile as well as conservative linear viscous shear zone models in 1D. These models need to be extended to more complexity as 2-dimensions or assumptions like power-law viscous fluid flow, which would result in a more natural shear stress evolution. Moreover, the results should be reproduced using additional shear zone profiles of the same scale and detailed sampling throughout various scales.

Appendix A

Related publications

This section aims to enumerate the publications and conference contributions related to this dissertation.

A.1 Publications

Kaatz, L., Zertani, S., Moulas, E., John, T., Labrousse, L., Schmalholz, S. M., & Andersen, T. B. (2021). Widening of hydrous shear zones during incipient eclogitization of metastable dry and rigid lower crust — Holsnøy, western Norway. *Tectonics*, *40*(3), e2020TC006572. https://doi.org/10.1029/2020TC006572

Kaatz, L., Reynes, J., Hermann, J., & John, T. (2022). How fluid infiltrates dry crustal rocks during progressive eclogitization and shear zone formation: insights from H_2O contents in nominally anhydrous minerals. *Contributions to Mineralogy and Petrology*, *177*(7), 1-20. https://doi.org/10.1007/s00410-022-01938-1

Kaatz, L., Schmalholz, S. M., & John, T. (XXXX). Transient weakening during shear zone formation by diffusional hydrogen influx and H2O inflow – from field observation to numerical simulation. *In preparation to be submitted to: Geochemistry, Geophysics, Geosystems*

A.2 Conference contributions

Kaatz, L., Reynes, J., John, T., Schmalholz, S., Hermann, J., & Moulas, E. (2020). The distribution of the H_2O content in nominally anhydrous minerals and its effect on shear zone widening (Holsnøy, West-Norway). In *EGU General Assembly Conference Abstracts* (p. 8198).

Kaatz, L., Reynes, J., John, T., Hermann, J., Vrijmoed, H. J., Liesegang, M., & Schmalholz, S. (2021). The distribution of the H_2O content in nominally anhydrous minerals and its effect on shear zone formation and widening (Holsnøy, West-Norway). *Goldschmidt2021. Virtual. 4-9 July*.

Kaatz, L., Schmalholz, S. M., Reynes, J., Hermann, J., & John, T. (2022). H_2O contents in nominally anhydrous minerals and its effect on the formation of eclogite-facies, hydrous shear zones (Holsnøy, Western Norway). (No. EGU22-10147). *Copernicus Meetings*.

Kaatz, L., Schmalholz, S. M., Reynes, J., Hermann, J., & John, T. (2022). H_2O contents in nominally anhydrous minerals and its effect on the formation of eclogite-facies, hydrous shear zones (Holsnøy, Western Norway). *14th International Eclogite Conference*.

Appendix B

Supporting material of

*"*Widening of hydrous shear zones during incipient eclogitization of metastable dry and rigid lower crust – Holsnøy, Western Norway*"*

- Chapter 2

Appendix C

Supporting material of

*"*How fluid infiltrates dry crustal rocks during progressive

eclogitization and shear zone formation:

insights from H_2O contents in nominally anhydrous minerals*"*

- Chapter 3

Appendix D

Supporting material of

"Transient weakening during shear zone formation by diffusional hydrogen influx and H_2O influx – from field observation to umerical simulation"

- Chapter 4

Supplementary Text 4.1 – ST4.1

This supplementary material provides and explains how to use the numerical codes utilized for 1D shear zone modelling (*Main_code.m*), viscosity mixing with W and H (*Eta_mix_H.mat* and *Eta_mix_W.mat*), visualization (*Visualization.m*), and post pure shear flattening (*Flattening.m*).

Main_code.m (run first)

This code provides the 1D shear zone model including all variations to run the code. Both influxes are implemented: aqueous fluid inflow (W) and hydrogen influx (H) based on the principles of continuum mechanics as described in section three. All steps are explained within the code using the commenting function. Furthermore, .mat files needed for further visualization or flattening are stored after each run automatically. Possible lines to change the initial values are as follows:

Line 8   : diffusivity of W
Line 12   : size of initial shear zone width
Line 16   : diffusivity ratio (to change D_H based on D_W)
Line 17 – 21   : if D_W is variable – uncomment, and adjust for a and b (see equation 5)
Line 30 – 34   : if D_H is variable – uncomment, and adjust for a and b (see equation 5)
Line 43   : weak viscosity
Line 47   : viscosity ration (to change the transition viscosity based on the weak viscosity)
Line 54 & 55   : change DW or DH to DW_var or DH_var, respectively,
                    if variable diffusivities are suggested
Line 63 & 64   : uncomment if variable DW or DH are suggested
Line 84 – 88   : uncomment if variable DW or DH are suggested
Line 113 – 116 : comment if variable DW is suggested
Line 117 – 121 : uncomment if variable DW is suggested
Line 122 – 125 : comment if variable DH is suggested
Line 126 – 130 : uncomment if variable DH is suggested
Line 177   : define output after X-timestep
Line 241 & 242: uncomment if variable DW or DH are suggested
Line 247 & 248: adjust if variable DW or DH are suggested

Eta_mix_H.mat, Eta_mix_W.mat

Viscosity mixing model using the Minimized Power Geometric (MPG) mixing model for viscously deforming polyphase rock of Huet et al., 2014.

Visualization.m

This code can be used to plot Figure 6 and Figure 7 hence, the evolution of parameters, e.g., W and H, normalized displacement, effective viscosity, and diffusivities. Adjust with respect to constant or variable D_W and D_H.

Flattening.m

Use to apply a pure shear component to the results of the *Main_code.m*. Adjust Line 13 and Line 15 to change the limits of flattening, area and strain, respectively.

Supplementary Table 4.2 – ST4.2 Raw-Data of the measured H_2O contents in grt, cpx and plg along the shear zone profile (data from Kaatz et al. 2022). These measurements were used to display and reproduce the hydrogen influx.

Garnet

points	distance [cm]	average H_2O – content [µg/g]	n (measurements per grain)
1	0.15	96.76	3
2	0.16	83.82	2
3	0.68	82.65	1
4	0.69	103.16	1
5	0.69	70.03	8
6	0.92	57.55	3
7	1.75	61.42	3
8	1.99	57.73	3
9	2.48	61.01	3
10	3.12	59.49	2
11	3.24	48.28	2
12	3.27	33.09	1
13	3.63	50.35	13
14	3.64	22.58	15
15	4.40	42.17	3
16	4.68	45.42	2
17	4.94	45.78	2
18	5.45	36.24	3
19	5.48	34.37	2
20	5.52	30.83	3
21	6.02	34.43	1
22	6.42	38.33	2
23	6.51	38.33	2
24	6.67	43.11	1
25	7.02	34.66	2
26	7.34	51.97	2
27	7.68	34.37	2
28	7.69	26.82	2
29	7.76	28.99	2
30	8.18	33.14	4
31	8.73	17.46	1
32	8.87	4.85	3
33	8.88	5.59	6
34	8.90	5.32	9
35	8.93	8.76	7
36	8.96	12.59	1
37	8.98	15.34	2
			$\sum$ 124

Clinopyroxene

points	distance [cm]	average H_2O – content [µg/g]	n (measurements per grain)
1	0.22	484.83	1
2	0.48	279.14	1
3	0.48	285.77	1
4	1.05	452.49	1
5	1.23	491.48	1
6	1.38	419.54	9
7	1.39	367.16	1
8	1.39	370.71	16
9	3.30	362.23	1
10	3.33	371.85	1
11	3.46	197.44	6
12	3.50	458.31	1
13	3.65	301.58	1
14	3.68	242.31	29
15	3.70	197.57	19
16	3.72	242.48	1
17	3.78	183.6	3
18	3.85	293.29	11
19	3.99	323.15	1
20	4.45	270.72	1
21	4.48	266.84	1
22	4.90	258.55	1
23	5.23	224.78	1
24	5.33	168.27	1
25	5.46	247.62	1
26	5.52	158.4	1
27	5.61	225.3	1
28	5.64	233.65	1
29	5.74	131.7	1
30	5.96	189	1
31	6.16	189.56	1
32	6.38	255	1
33	6.41	169.85	7
34	6.48	265.76	1
35	6.93	260.42	1
36	8.47	191.82	1
37	8.49	197.85	1
38	8.50	145.37	1
39	8.53	133.98	1
40	8.57	148.42	1
41	8.58	139.68	1
42	8.61	114.79	1
			$\sum$ 134

Plagioclase

points	distance [cm]	average H_2O – content [µg/g]	n (measurements per grain)
1	2.03	123.23	1
2	2.06	93.36	1
3	2.08	144	1
4	2.27	52.44	1
5	2.32	93.21	1
6	2.32	100.42	1
7	2.33	67.10	1
8	2.33	108.96	1
9	2.33	48.83	1
10	2.37	75.27	1
11	2.39	68.80	1
12	2.40	53.29	1
13	2.40	58.11	1
14	2.41	85.92	1
15	2.54	106.61	1
16	2.57	54.00	1
17	2.58	107.98	1
18	2.60	57.88	1
19	2.60	135.27	1
20	2.62	32.34	1
21	2.63	112.15	1
22	2.66	73.46	1
23	2.69	66.62	1
24	2.69	43.83	1
25	2.87	25.66	1
26	2.87	46.81	1
27	2.91	42.42	1
28	2.91	42.98	1
29	2.95	51.87	1
30	3.39	46.54	1
31	3.89	33.41	1
32	4.76	42.29	1
33	5.80	18.49	1
34	5.89	3.54	1
35	5.99	32.15	1
36	6.08	10.54	1
37	6.17	16.19	1
38	6.21	22.92	1
39	6.22	17.25	1
40	6.22	2.31	1
41	6.26	7.63	1
42	6.34	20.6	1
43	6.49	22.50	1
44	6.50	16.28	1
45	6.51	8.99	1

46	6.52	28.13	1
47	6.52	8.00	1
48	6.53	5.61	1
49	6.53	7.57	1
50	6.54	5.95	1
51	6.62	12.15	1
52	6.64	5.61	1
53	6.72	10.42	1
54	6.98	9.9	1
55	7.19	6.48	1
56	7.44	11.14	1
57	7.87	2.46	1
58	7.19	2.79	1
59	7.89	2.76	1
60	7.89	5.84	1
61	7.89	5.18	1
62	7.89	12.78	1
63	7.99	2.63	1
64	7.89	1.81	1
65	8.12	2.07	1
66	8.41	12.64	1
67	8.50	2.19	1
68	8.58	6.86	1
69	8.63	7.06	1
70	8.76	9.35	1
71	8.89	4.13	1
72	9.01	11.76	1
73	9.14	8.86	1
74	9.18	0.35	1
75	9.18	0.41	1
76	9.18	0.28	1
77	9.18	4.65	1
78	9.19	11.21	1
79	9.19	5.85	1
80	9.19	5.29	1
81	9.20	4.58	1
82	9.27	9.63	1
83	9.39	4.05	1
84	9.52	4.32	1
85	9.60	1.72	1
86	9.65	7.07	1
87	9.65	6.07	1
88	9.66	0.38	1
89	9.66	0.42	1
90	9.66	0.21	1
91	9.67	0.41	1
92	9.71	4.31	1
93	9.76	4.18	1

94	9.78	5.63	1
95	9.82	11.22	1
96	9.87	5.63	1
97	9.93	3.36	1
98	9.98	2.41	1
99	10.04	1.75	1
100	10.09	7.65	1
101	10.10	2.03	1
102	10.15	0.45	1
103	10.20	0.72	1
104	10.26	0.41	1
			∑ 104

Supplementary Table S4.3 – ST4.2 Raw-Data of the modal abundance of granulite- and eclogite-facies phases along the shear zone profile measured in separated segments (given in Vol.%, data used from Kaatz et al. 2022). Normalized values represent the H_2O-influx/eclogitization. Abbreviations: grt = Garnet, cpx = Clinopyroxene, oomph = Omphacite, plg = Plagioclase, czs = Cllinozoisite, amph = amphibole.

distance [cm]	grt	granulitic cpx	omph	plg	albite-rich plg	czs	amph	others	granulite-facies phases	eclogite-facies phases
0 – 1.5	28.4	8.5	9.7	17.4	17.6	10.4	2.7	5.5	40	60
1.5 – 2.5	19.3	7.2	5.1	35.3	16.9	9.8	2.3	4.2	52	48
2.5 – 3.7	18.7	7.9	0.8	44.8	13.0	11.8	1.3	1.7	62	38
3.7 – 5.1	22.7	11.7	0.2	55.8	3.0	5.3	0.6	0.6	79	21
5.2 – 6.7	25.6	11.5	0.7	60.2	0.6	0.7	0.2	0.5	84	16
6.7 – 9.2	23.2	14.1	0.1	60.5	0.1	1.5	0.2	0.2	86	14

Supplementary Table 4.4 – ST4.4 Porosity data raw data. Two sample were measured using steady state pore volume method. This method was not suitable for the granulite sample, which is why an automated unsteady state (CMS-300) was used. Subsequently, porosity data for 2.0 GPa was recalculated using the raw data.

	Net Confining Stress (psig)	Pore Volume (cm3)	Porosity (%)
Steady state pore volume			
Ec. shear zone	15	0.137	2.325
Ec. shear zone	1450	0.135	2.290
Ec. shear zone	3625	0.126	2.137
Ec. shear zone	5800	0.115	1.962
Ec. shear zone	7980	0.107	1.827
Ec. shear zone	9000	0.106	1.808
transition zone	15	0.244	2.367
transition zone	1450	0.191	1.859
transition zone	3625	0.164	1.603
transition zone	5800	0.136	1.332
transition zone	7980	0.125	1.221
transition zone	9000	0.122	1.200
Automated unsteady state_CMS-300			
granulite	1450	0.236	2.495
granulite	3625	0.211	2.239
granulite	5800	0.205	2.172
granulite	7980	0.195	2.070
granulite	9000	0.193	2.051

150

Acknowledgements

Furthermore, I like to thank my family and an indescribable gratitude goes to my friends, which are a lot more than that. Thank you for your encouragement, support, love, and friendship that helped me through the last years and especially, the last month. Unfortunately, I can name all but at least a few: Annemarie, Paula, Florian, Aileen, Marie, Stephi, Luis, Eric, Anika, Lemmi, Hanni, Paul W., Klexi, Kim, Steffi, Paul W.2, Ron, Theres, Patty, Lena, Karl, Benno, Chris, Anna, Loreen….

Finally, I want to thank my love Vinzent. Thank you for your unlimited support, listening me complaining, and being ebulliently positive again and again. Thank you for constant motivation and being just you.